

**Isolation and Structure Determination of New Compounds
from *Baeckea frutescens* Collected in Indonesia and Their
Antibacterial and Cytotoxic Activities**

KHOIRUN NISA

DIVISION OF NATURAL PRODUCTS CHEMISTRY

INSTITUTE OF NATURAL MEDICINE

UNIVERSITY OF TOYAMA

2016

Table of contents

Abbreviations	1
Introduction.....	3
Chapter 1 Antibacterial Screening of Indonesian Medicinal Plants.....	6
1.1. Introduction.....	6
1.2. Antibacterial Assay Screening	10
1.3. Summary of Chapter 1.....	11
Chapter 2 Constituents of the Leaves of <i>Baeckea frutescens</i> Collected in Indonesia	12
2.1. Introduction.....	12
2.2. Extraction and isolation procedure	14
2.3. Structure Elucidation of New Compounds.....	18
2.3.1. Structure of baeckenone A (1)	18
2.3.2. Structure of baeckenones B (2) and C (3)	21
2.3.3. Structure of baeckenones D (4) and E (5)	26
2.3.4. Structure of baeckenone F (6).....	33
2.3.5. Structure of frutescencenones A (7) and B (8).....	36
2.3.6. Structure of frutescencenone C (9).....	43
2.3.7. Structure of baeckenones G (10) and H (11).....	46
2.3.8. Structure of baeckenone I (12).....	52
2.4. Summary of Chapter 2.....	55
Chapter 3 Biological Activities of Constituents Isolated from <i>Baeckea frutescens</i>	56
3.1. Introduction.....	56

3.2. Antibacterial Activities of Compounds Isolated from the leaves of <i>B. frutescens</i>	57
3.3. Cytotoxic activity of Isolated from the leaves <i>B. frutescens</i>	58
3.4. Summary of Chapter 3.....	59
Conclusions.....	60
Experimental Section.....	62
I. General Experimental Procedures	62
II. Experimental Detail of Chapter 1	63
III. Experimental Detail of Chapter 2	65
IV. Experimental Detail of Chapter 3.....	70
References.....	72
List of publications.....	79
Acknowledgments	80

Abbreviations

$\mu\text{g/mL}$	Microgram per milliliter
μL	Micro liter
μM	Micro molar
$^{13}\text{C NMR}$	Carbon Nuclear Magnetic Resonance
$^1\text{H NMR}$	Proton Nuclear Magnetic Resonance
A549	Human lung cancer cell line
calcd	Calculated
CDCl_3	Deuterated chloroform
CH_3	Methyl
CH_3CN	Acetonitrile
CHCl_3	Chloroform
CO_2	Carbondioxide
COSY	Correlation Spectroscopy
D MEM	Dubelco's Modified Eagle's Medium
DMSO	Dimethylsulfoxide
EtOAc	Ethyl acetate
g	Gram
H_2O	Water
HMBC	Heteronuclear Multiple Bond Correlation
HMQC	Heteronuclear Multiple Quantum Correlation
HPLC	High Performance Liquid Chromatography
HREIMS	High Resolution Electron Impact Mass Spectrometry
HRESIMS	High Resolution Electron Spray Ionization Mass Spectrometry
IC_{50}	Concentration of inhibitory causing 50% reduction in activity relative to the control
IR	Infrared
J	Coupling constant

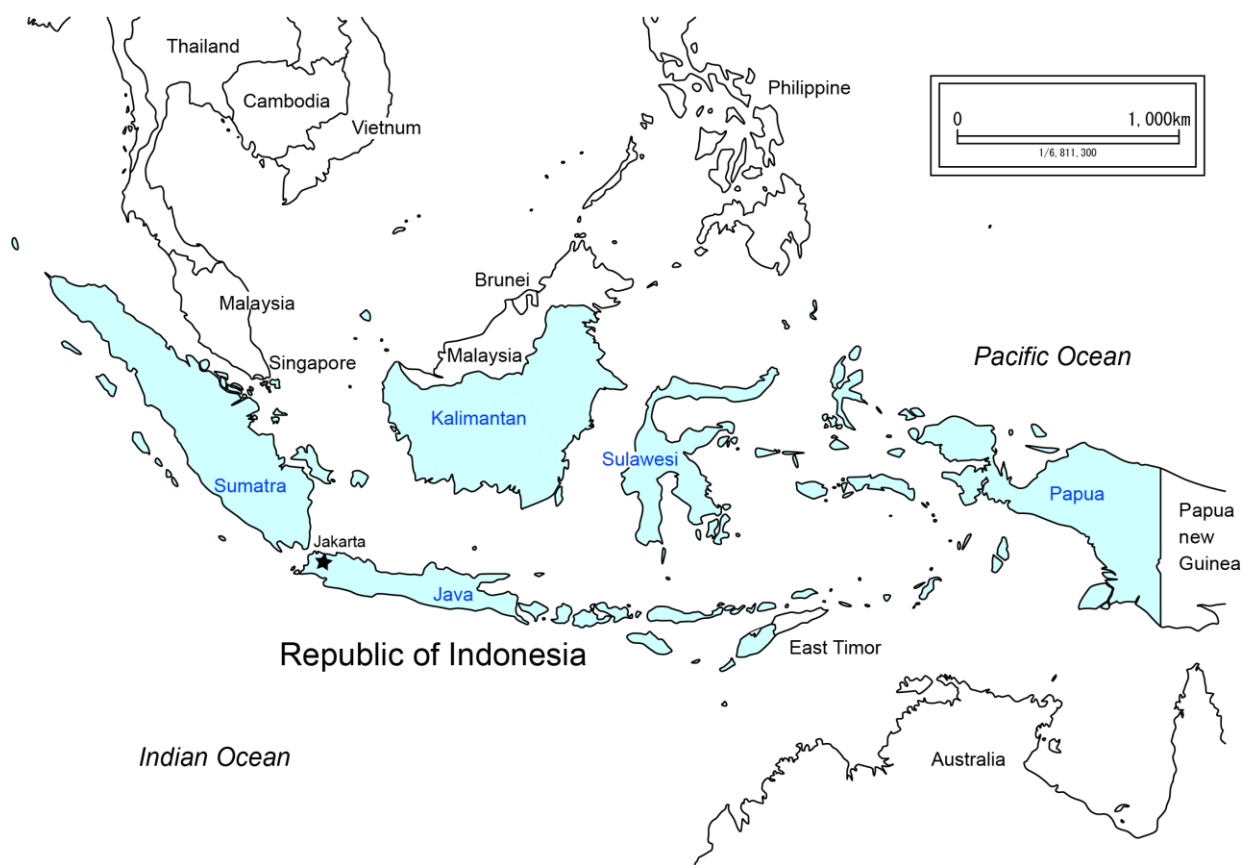
<i>m/z</i>	Mass-to-charge ratio
MDA-MB231	Human breast cancer cell line
MeOH	Methanol
mg	Milligram
MgSO ₄ ·7H ₂ O	Magnesium sulfate heptahydrate
MHz	Megahertz
MIC	Minimum inhibitory concentration
min	Minute
mm	Millimeter
mM	Millimolar
MPLC	Medium Pressure Liquid Chromatography
MS	Mass Spectroscopy
MTT	3-(4,5-dimethylthiazol-2-yl)-2,5-diphenyl tetrazolium bromide
mult	Multiplicity
NMR	Nuclear Magnetic Resonance
NOESY	Nuclear Overhauser Effect Spectroscopy
OCH ₃	Methoxy
OH	Hydroxy
PBS	Phosphate buffered saline
PSN-1	Human pancreatic cancer cell line
RP	Reversed Phase
TLC	Thin Layer Chromatography
TMS	Tetramethylsilane
UV	Ultra Violet
YP	Yeast extract Peptone
α-MEM	Minimum Essential Medium α

Introduction

Products origin from nature, called natural products, have been taken part in ancient traditional medicine systems, such as Traditional Chinese Medicine (TCM), Ayurveda, and Japanese Kampo medicine as well as in common use today. Natural products, particularly medicinal plants, have been used as traditional medicine for centuries and gaining much attention among the public and researchers due to the fact that they are natural, affordable, less toxic, and readily accessible.¹ According to the World Health Organization (WHO) report, 80% of people still rely on plant-based traditional medicines for primary health care globally.² The medicinal plants not only provide a wide range of vitamins and nutrients to the human diet, but also possess chemical compounds, which might have the potential as therapeutic agents.³ There are many compounds used in medicine today whose original derivatives were from plant origin. Thus, natural products will continue to serve as the basis of new drugs in the years to come because natural products offer incomparable structural diversity, relatively small molecules (< 2000 Da), and have “drug-like” properties. In addition, natural products have an important feature, which often shows highly selective and specific biological activities based on mechanisms of action. Strategies for research in the area of natural products have evolved quite significantly over the last few decades.⁴

Indonesian archipelago is comprised of more than 18,000 islands, including Sumatra, Java, Kalimantan, and Sulawesi. Straddling the equator, Indonesia has a tropical climate characterized by heavy rainfall, high humidity, and high temperature. Around two-thirds of the area in Indonesia is generally covered with tropical rainforests. Therefore, Indonesia has a

various type of ecological system as well as high levels of biodiversity in the world. Over 38,000 species of tropical plants have been found in Indonesia. Among them, 7,000 species of medicinal plants have been used as Indonesian traditional medicine, “Jamu”.⁵ A great number of biologically active metabolites have been reported from Indonesian medicinal plants during a couple of decades. However, most of natural product resources have remained to be fully investigated. Thus, the search for novel bioactive constituents from Indonesian medicinal plants still attracts our attention for the discovery and development of new drugs.



Infectious diseases are the world's leading cause of human deaths. The discovery of antibiotics has decreased the spread and severity of a variety of infectious diseases.⁶ However, the outbreak of drug resistant microorganism become the great problem in the world.⁷ Therefore, the developing of alternative antimicrobial drugs for the treatment of infectious diseases are now required. Considering the failure to gain new molecules with antimicrobial properties from microorganisms, the screening methods used for the identification of antimicrobials from other natural sources is of great worth.⁸ In recent times, the search for potent antimicrobial agents has been shifted to the medicinal plants. There are many published reports on the effectiveness of medicinal plants against Gram-positive and Gram-negative bacteria. Therefore, plants are recognized as the basis for modern medicine to treat infectious diseases and also taken up as the important source for the discovery of new antibiotics.^{9,10}

This study aims to isolate new compounds from *Baeckea frutescens* leaves, by focusing on antibacterial and cytotoxic activities. Chapter 1 provides a preliminary screening study of several medicinal plants collected in Indonesia based on antibacterial activity. Antibacterial activity of crude extracts was examined against Gram-positive and Gram-negative bacteria. In Chapter 2, according to the result of previous chapter, I discuss about the isolation and structure elucidation of new compounds from *B. frutescens*. Finally, Chapter 3 describes the antibacterial and cytotoxic activities of the constituents isolated from *B. frutescens*.

Chapter 1 Antibacterial Screening of Indonesian Medicinal Plants

1.1. Introduction

Recently, the emergence of new infectious diseases and the increase of bacterial resistance create the importance of new antimicrobials discovery.¹¹ The increasing demand of plant-based antimicrobial agents led to the screening of antibacterial activity from twenty-six Indonesian medicinal plants (Table 1.1).

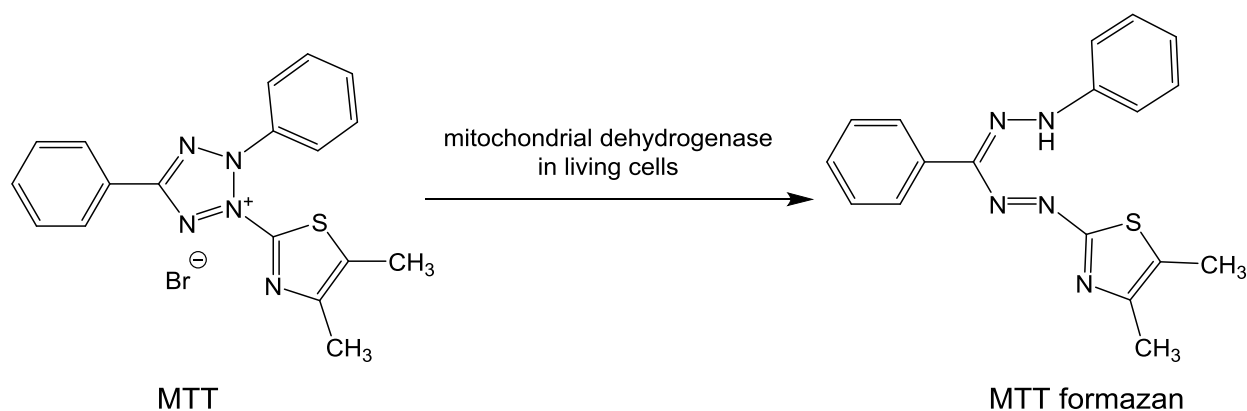


Figure 1.1. MTT reaction scheme

The screening methods to determine antimicrobial activity of natural products are mainly divided into three groups, bio-autographic, diffusion, and dilution methods. Among them, the dilution method is a quantitative assay that is able to determine the minimum inhibitory concentration (MIC).¹² The dilution method combined with MTT (3-(4,5-dimethylthiazolyl-2)-2,5-diphenyltetrazolium bromide) reduction assay is one of the most frequently used methods for measuring antibacterial activity. This method has been recently developed as a rapid

colorimetric assay to test the antibacterial susceptibility of various synthetic and natural remedies.¹³ MTT is reduced by mitochondrial dehydrogenase in living cells to produce insoluble purple MTT formazan, which can be spectrophotometrically measured upon solubilization.¹⁴ This method presents high sensitivity, versatile, and quantitative, and turns into a significant advance over traditional techniques for several commonly used antimicrobial assays.

Table 1.1. Selected Indonesian medicinal plants and their family, part used, local name, and therapeutic applications

No.	Botanical name	Family	Part used	Local name	Therapeutic used
1.	<i>Phyllanthus reticulatus</i> Poir.	Euphorbiaceae	Fruit	Mangsi-an	Anti-inflammatory
2.	<i>Blumea balsamifera</i> (L.) DC.	Asteraceae	Leaf	Sambung	Cold, diuretic
3.	<i>Mischocarpus sundaicus</i> Blume	Sapindaceae	Leaf	Dandang gulo	Cough
4.	<i>Baeckea frutescens</i> L.	Myrtaceae	Leaf	Jungrahab	Malaria, rheumatism
5.	<i>Euchresta horsfieldii</i> (Lesch.) Benn.	Fabaceae		Prono jiwo solo	Hyperlipidemia
6.	<i>Clerodendrum serratum</i> (L.) Moon	Verbenaceae	Root	Senggugu	Dyspepsia, rheumatism
7.	<i>Litsea cubeba</i> (Lour) Pers.	Lauraceae	Bark	Krangean	Asthma, dermatitis
8.	<i>Parameria laevigata</i> (Juss.) Moldenke	Apocynaceae	Bark	Kayu rapet	Dysentery, tuberculosis
9.	<i>Nyctanthes arbor-tristis</i> Linn.	Oleaceae	Flower	Srigading	Dysmenorrheal
10.	<i>Gynura procumbens</i> (Lour.) Merr.	Asteraceae	Bulb	Sambung nyowo	Diabetes, hypertension
11.	<i>Cryptocaria massoia</i> (Oken) Kosterm.	Lauraceae	Bark	Mesoyi	Antispasmodic, tonic
12.	<i>Stelechocarpus burahol</i> Hook. f. & Thomson	Annonaceae	Leaf	Kepel	Hyperuricemia, anticholesterol
13.	<i>Quercus infectoria</i> Oliv.	Fagaceae	Seed	Manjakani	Chronic diarrhea, uterine disorders
14.	<i>Abelmoschus moschatus</i> (L.) Medic	Malvaceae	Seed	Regulo solo	Muscle spasms, gonorrhea
15.	<i>Elaeocarpus grandiflorus</i> Sm	Elaeocarpaceae	Bark	Anyang	Ulcers, headache
16.	<i>Woodfordia fruticosa</i> (L.) Kurz	Lythraceae	Flower	Sidowayah	Gout, skin disease
17.	<i>Justicia gendarussa</i> Burm F.	Acanthaceae	Leaf	Gandarusa	Earache, paralysis, antispasmodic

Table 1.1. (Continued)

No.	Botanical name	Family	Part used	Local name	Therapeutic used
18.	<i>Selaginella doederleinii</i> Hieron	Selaginellaceae	Leaf	Cakar ayam	Pneumonia, lung cancer, hepatitis, cough
19.	<i>Murraya paniculata</i> (L.) Jack	Rutaceae	Leaf	Kemuning	Analgesic
20.	<i>Curcuma mangga</i> Valetton & van Zijp	Zingiberaceae	Rhizome	Temu Mangga	Asthma, cancer, bronchitis, fever
21.	<i>Alyxia reinwardtii</i> Blume	Apocynaceae	Bark	Pulosari	Colic, fever, dysentery
22.	<i>Hedyotis corymbosa</i> L.	Rubiaceae	Leaf	Rumput Mutiara	Bronchitis, hepatitis
23.	<i>Equisetum debile</i> Roxb.	Equicetaceae	Leaf	Greges Otot	Hepatitis, influenza, fever, dysentery
24.	<i>Erythrina variegata</i> L.	Fabaceae	Leaf	Cangkring	Dysentery, mastitis
25.	<i>Acanthus ilicifolius</i> L.	Acanthaceae	Leaf	Deruju	Dyspepsia, paralysis
26.	<i>Clerodendron serratum</i> (L.) Moon	Verbenaceae	Leaf	Senggugu	Asthma, allergy, fever

1.2. Antibacterial Assay Screening

Twenty-six Indonesian medicinal plants were extracted with MeOH and CHCl₃ to obtain the corresponding crude extracts. These extracts were screened for their antibacterial activities against three Gram-positive bacterial strains, *Bacillus subtilis* NBRC 3134, *Staphylococcus aureus* NBRC 15035, and *Mycobacterium smegmatis* NBRC 3082, and two Gram-negative bacterial strains, *Escherichia coli* NBRC 102203 and *Klebsiella pneumoniae* NBRC 3512 using the standard MTT assay.¹⁴ The minimum inhibitory concentration (MIC) value of the crude extracts was defined as the lowest concentration showed no visible bacterial growth after incubation at 37°C for 24 h. The investigated plant extracts showed no significant antibacterial activity against Gram-negative bacterial strain in concentration of 200 µg/mL. Among the crude extracts investigated, the CHCl₃ extract of *B. frutescens* leaves showed the antibacterial activities against *S. aureus* and *B. subtilis* with MIC values of 100 µg/mL and 200 µg/mL, respectively, while the CHCl₃ extract of *C. mangga* rhizome exhibited significant antibacterial activities against *B. subtilis* and *S. aureus* with MIC values of 150 µg/mL and 200 µg/mL, respectively. This screening result indicated that *B. frutescens* and *C. mangga* possessed antibacterial properties mainly against Gram-positive bacterial strains, *S. aureus* and *B. subtilis*, suggesting that Gram-positive bacteria is more susceptibility towards both plants extracts as compared with Gram-negative bacteria. These differences may be attributed to fact that the cell wall in Gram-positive bacteria has a single and much thicker peptidoglycan layer, whereas the Gram-negative cell wall is multilayered structure. The outer membrane of Gram-negative bacteria is composed of lipopolysaccharides, which is preventing the access of the drugs in the cells and also causing the antibiotic resistance of the bacteria.¹⁵

Table 1.2. Antibacterial activities of CHCl₃ extracts of *B. frutescens* and *C. mangga*

Plant extracts	MIC (µg/mL)				
	<i>S. aureus</i>	<i>M. smegmatis</i>	<i>B. subtilis</i>	<i>K. pneumoniae</i>	<i>E. coli</i>
<i>B. frutescens</i>	100	> 200	200	> 200	> 200
<i>C. mangga</i>	200	> 200	150	> 200	> 200
Ampicillin ^a	0.1	0.1	0.1	0.1	0.1

^a Positive control

1.3. Summary of Chapter 1

The preliminary study of antibacterial activity for twenty-six Indonesian medicinal plants was investigated against several bacterial strains. Among them, the leaves of *B. frutescens* showed good antibacterial activities against Gram-positive bacteria, *S. aureus* and *B. subtilis* with MIC values of 100 µg/mL and 200 µg/mL, respectively. In contrast, *C. mangga* rhizome exhibited antibacterial activities against *S. aureus* and *B. subtilis* with MIC values of 200 µg/mL and 150 µg/mL, respectively. However, all plant extracts showed no significant activity against Gram-negative bacterial strains.

Chapter 2 Constituents of the Leaves of *Baeckea frutescens* Collected in Indonesia

2.1. Introduction

Baeckea frutescens L. of the family Myrtaceae is a small tree, which is originally found in Peninsular Malaysia, Sumatra, and the coastal areas of southern China and Australia. *B. frutescens* is the only species of genus *Baeckea* in Indonesia.¹⁶ *B. frutescens*, popularly known as “Jungrahab”, is commonly used in Indonesian folk medicine.¹⁷ Traditionally, the aerial parts of *B. frutescens* are employed as remedy for influenza, malaria, fever, headache, abdominal pain, and dysentery.^{18,19} Furthermore, *B. frutescens* has been reported to be effective in external usage such as rheumatism and snake bites in Hong Kong.²⁰ *B. frutescens* is found on top of mountain, quartz ridge, and sandy coasts of the eastern parts. This plant has a small, needle-like and narrow 6-15 mm long leaves. The leaves have a resinous aromatic fragrance when crushed and the flowers are minute, solitary or in pairs with white petals.²¹ Several studies reported the chemical composition of the essential oil obtained from *B. frutescens* leaves such as pinenes, α -terpinenes, limonene, linalool, *p*-cymene, α -terpineol, α -caryophyllene, and α -humulene.²² It also yielded many series of cyclic polyketones such as tasmanones and its derivatives.²³⁻²⁴ Many phytochemical constituents have been isolated from *B. frutescens* including sesquiterpenes, flavonoids, flavanones, phloroglucinols, chromones, and chromanones.²³⁻³⁵ Previous studies of this plant reported anti-inflammatory, antipyretic, antidiysenteric, antibacterial, and cytotoxic activities. However, only a few of them displayed biological effects such as antibacterial, anti-inflammatory, anti-arteriosclerosis, and cytotoxic activity.²³⁻²⁸

In continuation of this study, the phytochemical investigation of the CHCl_3 extract of *B. frutescens* leaves were carried out and led to the isolation of twenty-two compounds (**1-22**), including twelve new compounds (**1-12**).

a)



b)



Figure 2.1. *Baeckea frutescens* L. a) plant, b) leaves

2.2. Extraction and isolation procedure

The dried leaves of *B. frutescens* (425 g) were pulverized into a fine powder which was exhaustively extracted with CHCl₃ (3 × 1.5 L) in an ultrasonic bath for 90 min at room temperature. The resulting solution was evaporated under reduced pressure to yield the CHCl₃ extract (41 g) (Chart 1). The CHCl₃ extract was initially fractionated by normal phase medium pressure liquid chromatography (MPLC; 1.85 kg; 40-50 μm; 100 × 460 mm; flow rate = 25 mL/min) eluting with *n*-hexane and ethyl acetate by gradually increasing polarity system to yield 10 fractions (Fr.1–Fr.10). These fractions were further separated by repeated normal phase, reversed-phase, and Sephadex LH-20 column chromatographies, followed by purification using normal and reversed-phase preparative TLCs to afford twelve new compounds (**1–12**) (Figure 2.2) and ten known compounds (**13–22**) (Figure 2.3). All compounds were structurally elucidated on the basis of spectroscopic analyses and the known compounds were identified by comparison of their MS and NMR data with those reported in the literature to be baeckeol (**13**)²⁴, peroxide phloroglucinol (**14**)²⁰, cyclopentenone derivative (**15**)²⁰, cycloalkenone derivative (**16**)³⁵, 5,7-dihydroxy-6,8-dimethylflavanone (**17**)^{36,37}, 5,7-dihydroxy-6-methylflavanone (**18**)³⁷, 5,7-dihydroxy-8-methyl-6-prenylated flavanone (**19**)^{38,39}, hybrid phloroglucinol (**20**)²⁰, humulene diepoxide (**21**)⁴⁰, and ursolic acid (**22**)^{41,42}.

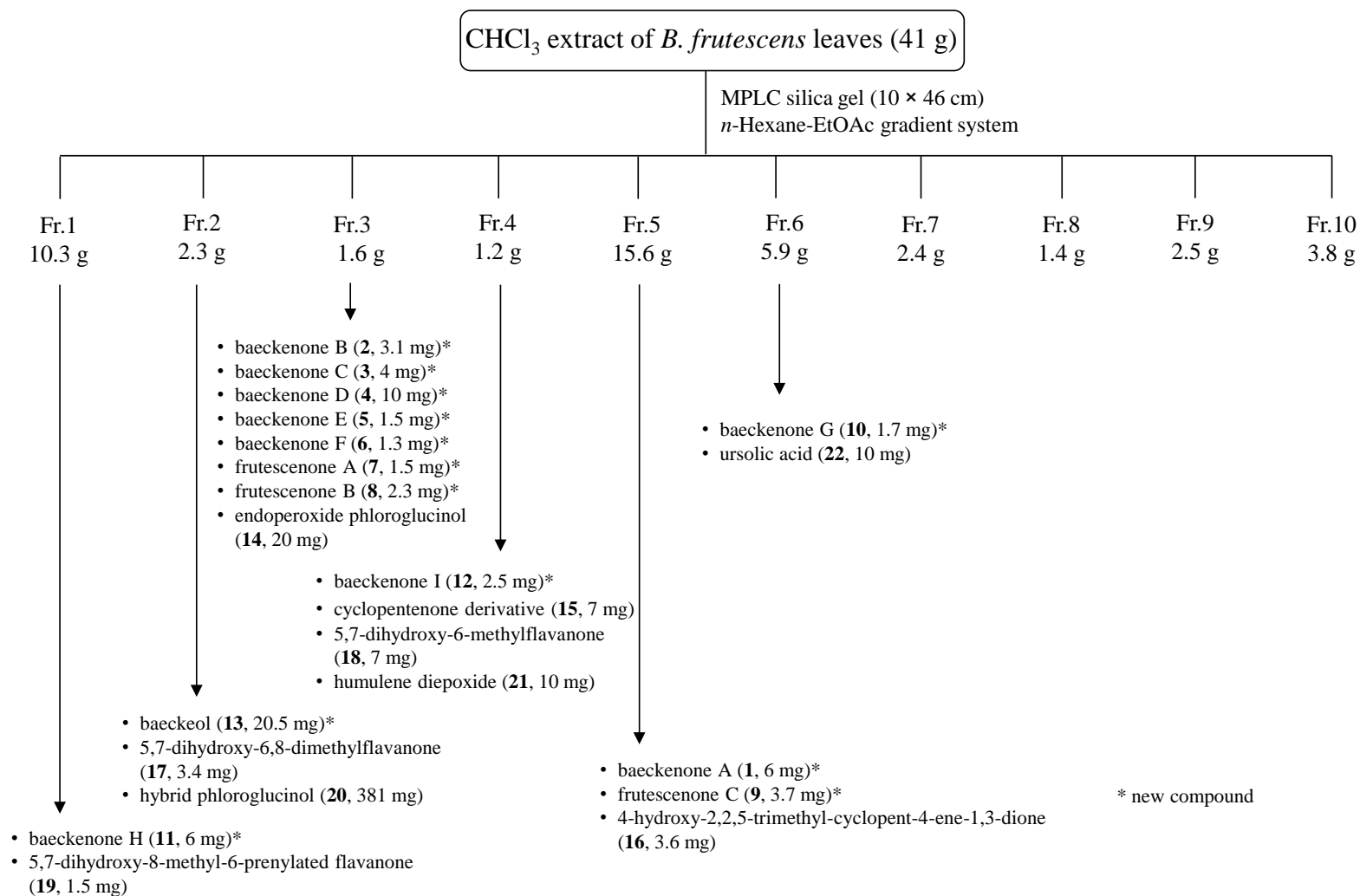


Chart 1. Isolation procedure of the CHCl₃ extract of *B. frutescens*

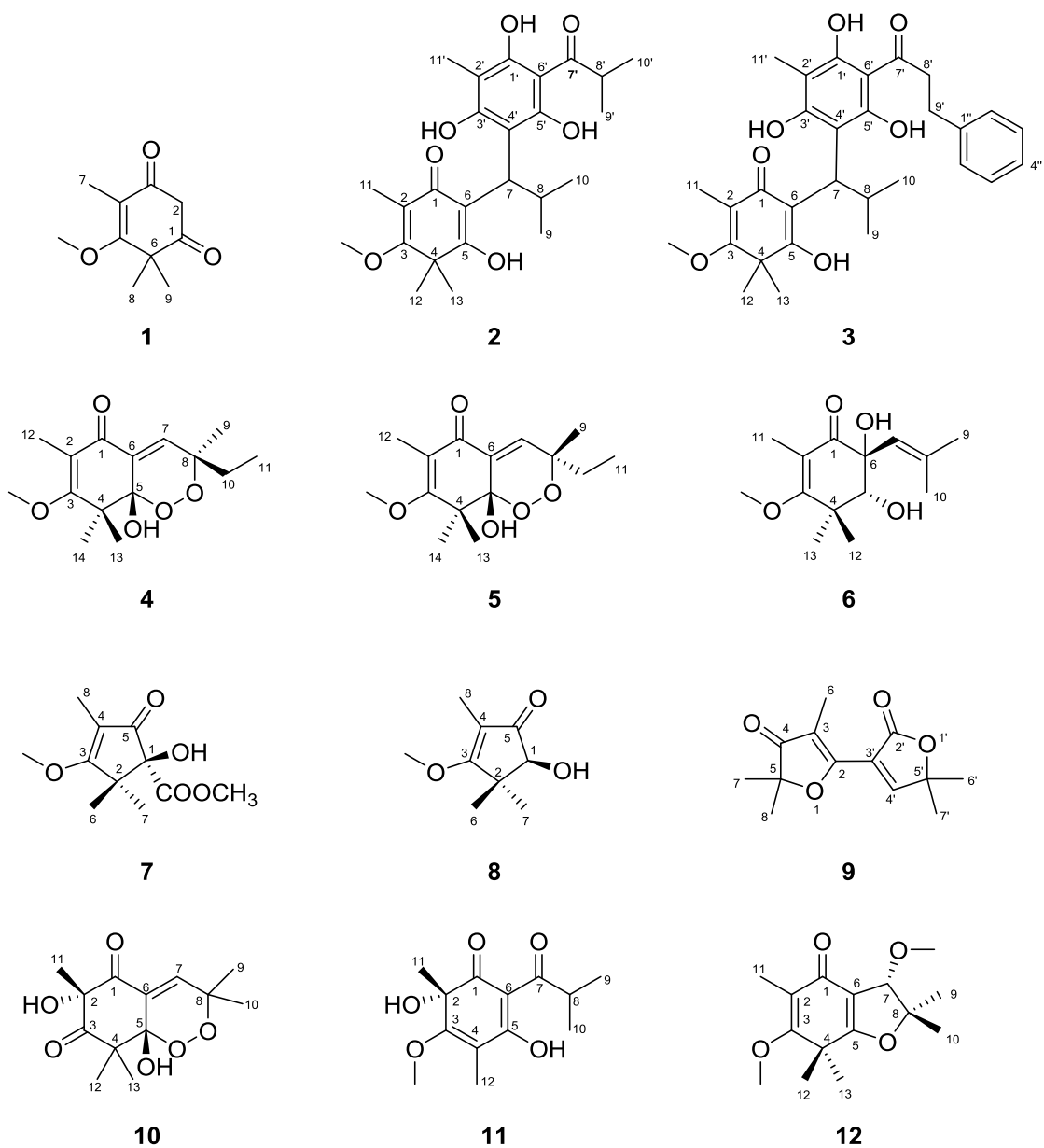


Figure 2.2. Structure of new compounds isolated from the CHCl_3 extract of *B. frutescens* leaves

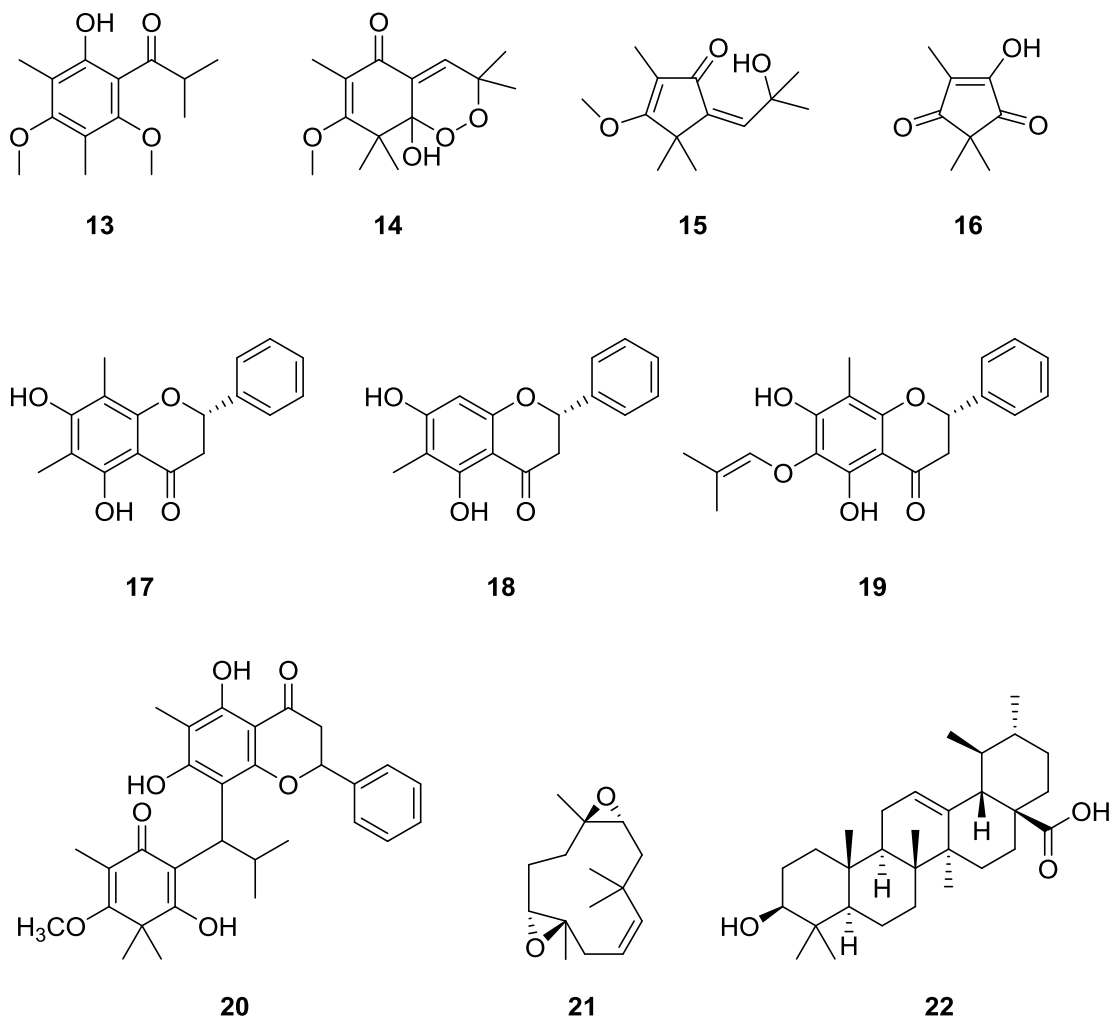


Figure 2.3. Structure of known compounds isolated from the CHCl_3 extract of *B. frutescens* leaves

2.3. Structure Elucidation of New Compounds

2.3.1. Structure of baeckenone A (**1**)

Compound **1** was obtained as a yellow amorphous powder. The HREIMS of **1** indicated a molecular ion peak at m/z 182 $[M]^+$, and the molecular formula $C_{10}H_{14}O_3$ was deduced as from HREIMS in conjunction with ^{13}C NMR data. The IR spectrum of **1** showed the absorbance band corresponding to a conjugated carbonyl group (1660 cm^{-1}). The combination analysis of 1H NMR and HMQC data (Table 2.1, Figure 2.4) displayed the presence of one methoxy group [δ_H 3.96 (s)], one allylic methyl group [δ_H 1.92 (s)], one methylene [δ_H 3.54 (s)], and two overlapped singlets of tertiary methyl groups [6H, δ_H 1.40 (s, overlapped)]. The ^{13}C NMR data (Table 2.1) revealed ten carbon signals attributable to two carbonyl carbons (δ_C 205.8, 192.8), two olefinic carbons (δ_C 177.5, 118.6), one methylene carbon (δ_C 51.0), one methoxy carbon (δ_C 62.2), one quaternary carbon (δ_C 51.7), and three methyl carbons (δ_C 22.8, 22.8, 10.3). The HMBC correlations from the *gem*-dimethyl groups at H₃-8 and H₃-9 (6H, δ_H 1.40) to C-6 (δ_C 51.7), C-1 (δ_C 205.8), and C-5 (δ_C 177.5) revealed that the *gem*-dimethyl groups were attached to the quaternary carbon at C-6 (Figure 2.5). Furthermore, the HMBC correlations from H₃-7 (δ_H 1.92) to C-4 (δ_C 118.6), C-3 (δ_C 192.8), and C-5 (δ_C 177.5) and from 5-OCH₃ (δ_H 3.96) to C-5 (δ_C 177.5) indicated the presence of carbonyl, methyl, and methoxy groups located at C-3, C-4, and C-5, respectively. Further analysis of the remaining HMBC correlations from H₂-2 (δ_H 3.54) to C-1 (δ_C 205.8) and C-3 (δ_C 192.8) allowed us to locate the methylene group at C-2 (δ_C 51.0) between the two carbonyl groups. The structure of compound **1** was assigned as 5-methoxy-4,6,6-trimethylcyclohex-4-ene-1,3-dione, and was given the trivial name baeckenone A.

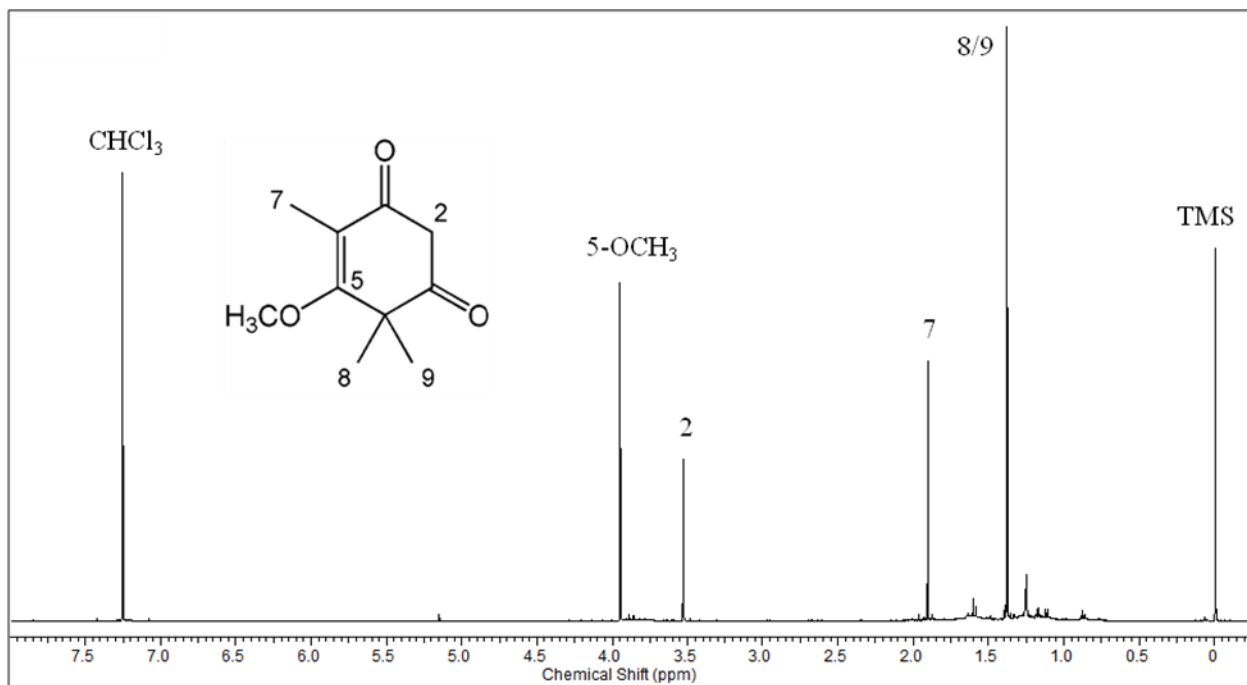


Figure 2.4. ^1H NMR spectrum of **1** in CDCl_3

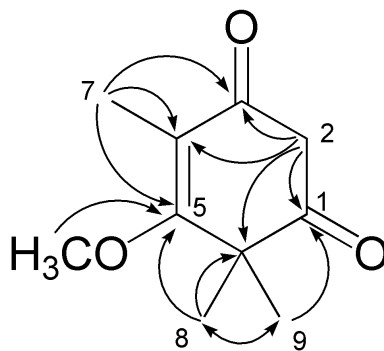


Figure 2.5. Key HMBC correlations (arrows) of **1**

Table 2.1. ^1H (600 MHz) and ^{13}C (150 MHz) NMR data for **1** in CDCl_3

Position	1	
	δ_{C}	δ_{H} (mult., J in Hz)
1	205.8	
2	51.0	3.54 (s)
3	192.8	
4	118.6	
5	177.5	
6	51.7	
7	10.3	1.92 (s)
8	22.8	1.40 (s)
9	22.8	1.40 (s)
5-OCH ₃	62.2	3.96 (s)

2.3.2. Structure of baeckenones B (**2**) and C (**3**)

Compound **2** was obtained as a yellow oil. Its HRESIMS exhibited a quasi-molecular ion peak at m/z 447.2383 $[M+H]^+$, corresponding to the molecular formula $C_{25}H_{35}O_7$ with eight degrees of unsaturation. The IR spectrum displayed strong absorption bands at 1614 cm^{-1} and 3419 cm^{-1} , assignable to carbonyl and hydroxyl groups, respectively. The ^1H NMR data of **2** (Table 2.2, Figure 2.6) revealed the signals for six aliphatic methyl protons [δ_{H} 1.41 (s), 1.31 (s), 1.22 (d, $J = 5.3$), 1.20 (d, $J = 5.3$), 0.81 (d, $J = 5.2$), 0.77 (d, $J = 5.2$)], two allylic methyl groups [δ_{H} 1.91 (s), 2.11 (s)], one methoxy group [δ_{H} 3.88 (s)], three methine protons [δ_{H} 3.96 (m), 3.78 (d, $J = 8.6$), 3.14 (m)], and four hydroxyl groups (δ_{H} 12.39, 11.33, 10.50, 9.69). The ^{13}C NMR (Table 2.2) and HMQC data revealed the presence of two ketone carbons (δ_{C} 210.9, 194.6), three oxygenated aromatic carbons (δ_{C} 162.1, 161.2, 155.4), two oxygenated olefinic carbons (δ_{C} 176.2, 174.4), five aromatic/olefinic quaternary carbons (δ_{C} 116.6, 113.8, 109.2, 102.7, 102.6), one methoxy group (δ_{C} 61.9), three methine carbons (δ_{C} 39.1, 38.9, 26.1), an aliphatic quaternary carbons (δ_{C} 43.9), and eight methyl groups (δ_{C} 23.8, 23.7, 22.0, 21.9, 19.5, 19.3, 9.8, 7.5). Analysis of the ^1H - ^1H COSY spectrum (Figure 2.7) led us to construct an isopropyl (C-8'/C-9'/C-10') and an isobutyl (C-7/C-8/C-9/C-10) groups in **2**. In the HMBC spectrum (Figure 2.7), correlations from H_3 -11' (δ_{H} 2.11) to C-1' (δ_{C} 155.4), C-2' (δ_{C} 102.6), and C-3' (δ_{C} 162.1), from H_3 -9' (δ_{H} 1.22) and H_3 -10' (δ_{H} 1.20) to C-7' (δ_{C} 210.9), from H-7 (δ_{H} 3.78) to C-3', C-4' (δ_{C} 109.2), and C-5' (δ_{C} 161.2), and from 3'-OH (δ_{H} 12.39) to C-2' and C-3' were observed (Figure 2.6). The 1D NMR data of these parts in **2** were similar to those of a known phloroglucinol, baeckeol (**13**), isolated from this plant in this study. This evidence

suggested that compound **2** possessed an isobutyryl phloroglucinol moiety, and an analogue of baeckeol (**13**) could be a biosynthetic intermediate of **2**. Furthermore, the HMBC correlations from H₃-11 (δ_{H} 1.91) to C-1 (δ_{C} 194.6), C-2 (δ_{C} 116.6), and C-3 (δ_{C} 174.4), from 3-OCH₃ (δ_{H} 3.88) to C-3, from H₃-12 (δ_{H} 1.41) and H₃-13 (δ_{H} 1.31) to C-3, C-4 (δ_{C} 43.9), and C-5 (δ_{C} 176.2), and from H-7 (δ_{H} 3.78) to C-1, C-5, and C-6 (δ_{C} 113.3) confirmed the existence of another isobutyl phloroglucinol moiety, and both of the phloroglucinol moieties were connected at C-7 and C-4'. Consequently, compound **2** was identified to be a new dimeric acylphloroglucinol and was named baeckenone B.

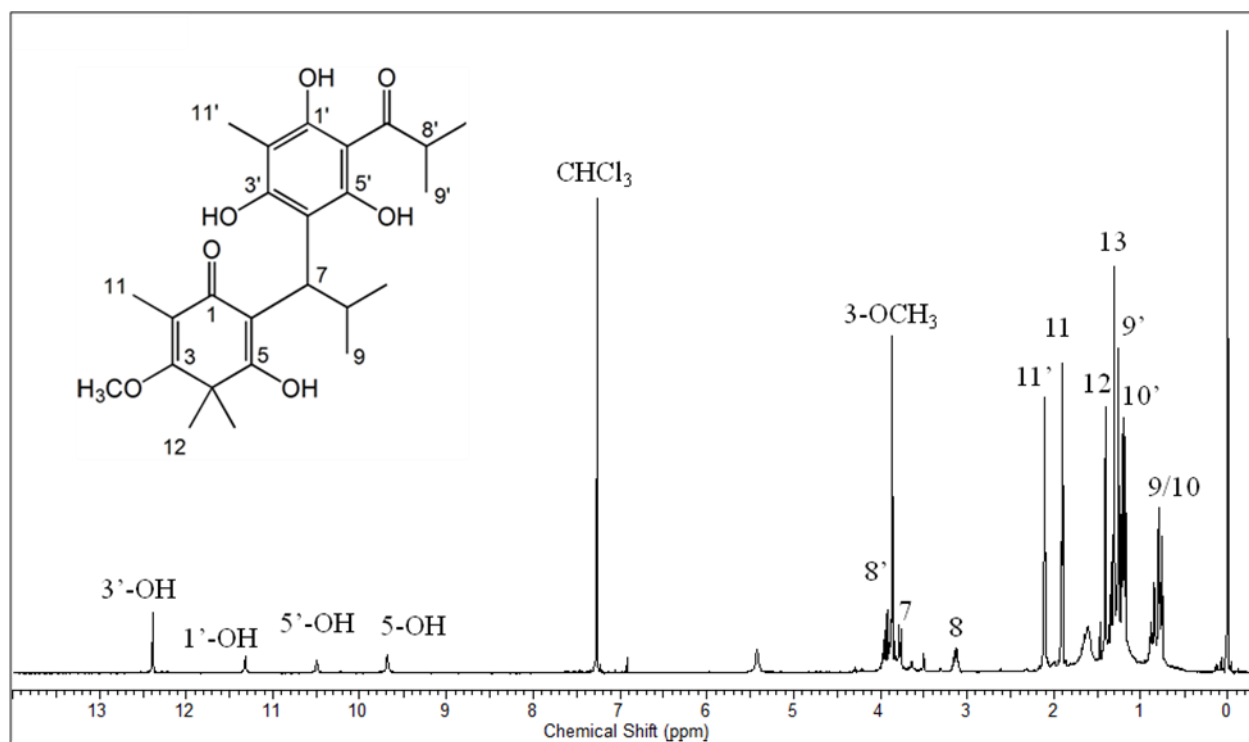


Figure 2.6. ¹H NMR spectrum of **2** in CDCl₃

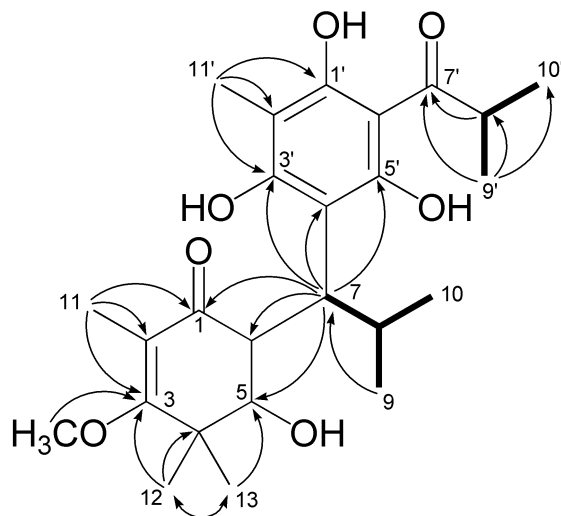


Figure 2.7. Key HMBC (arrows) and ^1H - ^1H COSY (bold lines) correlations of **2**

Compound **3** was obtained as a yellow oil, and its molecular formula was determined as $\text{C}_{30}\text{H}_{36}\text{O}_7$ by the HREIMS and ^{13}C NMR data. The IR spectrum displayed strong absorption bands for carbonyl (1617 cm^{-1}) and hydroxyl (3415 cm^{-1}) groups. The ^1H and ^{13}C NMR spectroscopic data of **3** (Table 2.2, Figure 2.8) were similar to those of **2**, except for the presence of a phenylethyl group [δ_{H} 3.44 (2H, t, $J = 8.3$, H_2 -8'), 3.03 (2H, t, $J = 8.3$, H_2 -9'), and 7.19–7.31 (5H, overlapped, H -2''–6'')] instead of the isopropyl group of **2**. The ^1H - ^1H COSY correlation between H_2 -8' and H_2 -9', as well as the HMBC correlations from H_2 -8' (δ_{H} 3.44) to C -7' (δ_{C} 205.1), C -9' (δ_{C} 30.8), and C -1'' (δ_{C} 141.6), and from H_2 -9' (δ_{H} 3.03) to C -7', C -8' (δ_{C} 45.4), C -1'', and C -2''/ C -6'' (δ_{C} 125.9) also supported that the phenylethyl group in **3** was linked to the carbonyl carbon (C -7') (Figure 2.9). Moreover, the 1D NMR data of **3** resembled closely those of a flavanone derivative (**20**). The major difference found between these compounds was that the oxygenated methine (C -9') in **20** was replaced by a benzylic methylene (δ_{H} 3.03; δ_{C} 30.8) in **3**. On the basis of these data, compound **3** was considered as the chalcone analogue of

20. Thus, compound **3** was elucidated as a new dimeric acylphloroglucinol, and was named baeckenone C.

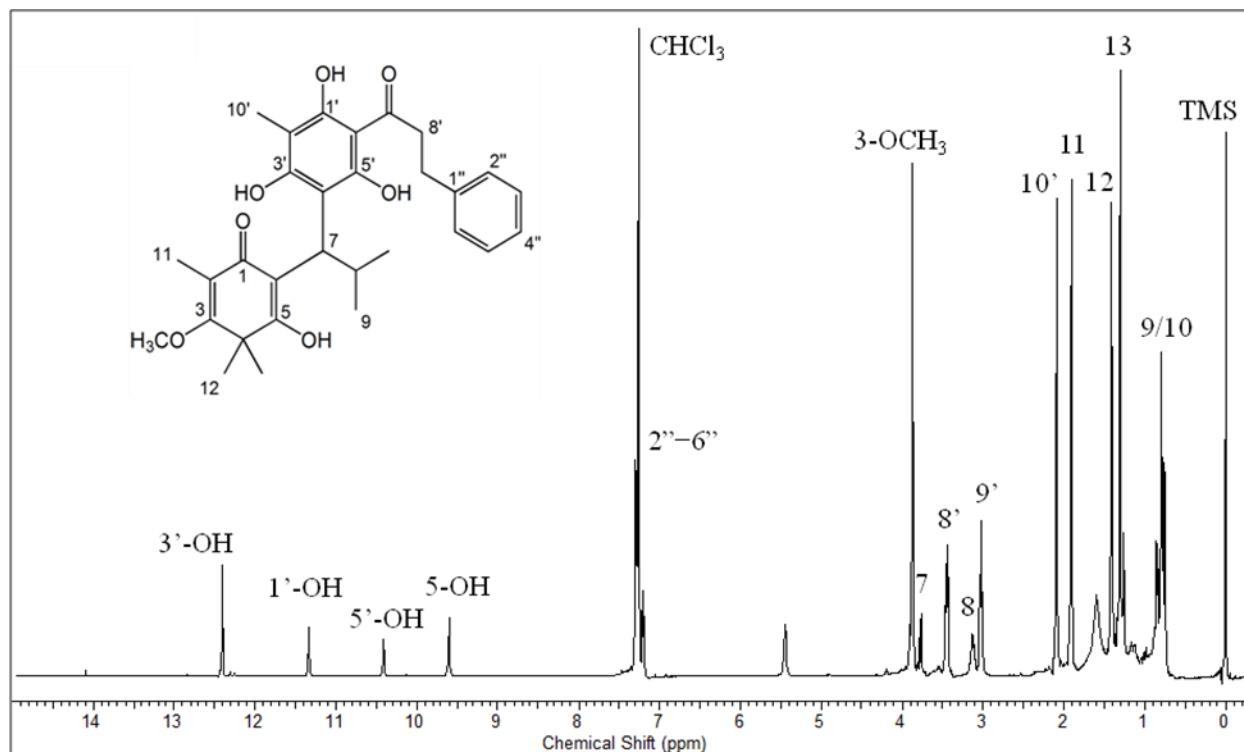


Figure 2.8. ^1H NMR spectrum of **3** in CDCl_3

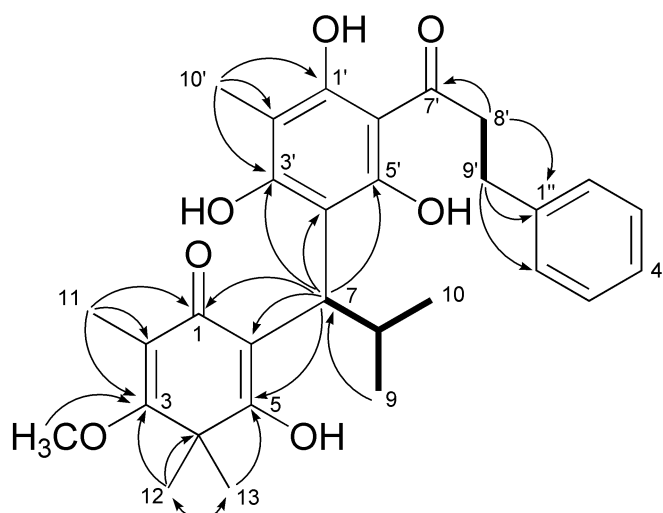


Figure 2.9. Key HMBC (arrows) and ^1H - ^1H COSY (bold lines) correlations of **3**

Table 2.2. ^1H (400 MHz) and ^{13}C (100 MHz) NMR data for **2** and **3** in CDCl_3

Position	2		3	
	δ_{C}	δ_{H} (mult., J in Hz)	δ_{C}	δ_{H} (mult., J in Hz)
1	194.6		191.7	
2	116.6		116.6	
3	174.4		174.4	
4	43.9		43.9	
5	176.2		175.6	
6	113.8		113.8	
7	39.1	3.78 (d, 8.6)	39.0	3.76 (d, 8.8)
8	26.1	3.14 (m)	26.1	3.13 (m)
9	22.0	0.81 (d, 5.2)	22.0	0.85 (d, 4.8)
10	21.9	0.77 (d, 5.2)	21.9	0.76 (d, 4.8)
11	9.8	1.91 (s)	9.9	1.91 (s)
12	23.8	1.41 (s)	24.0	1.41 (s)
13	23.7	1.31 (s)	23.9	1.30 (s)
1'	155.4		155.8	
2'	102.6		102.6	
3'	162.1		162.3	
4'	109.2		109.1	
5'	161.2		160.6	
6'	102.7		103.2	
7'	210.9		205.1	
8'	38.9	3.96 (m)	45.4	3.44 (t, 8.3)
9'	19.5	1.22 (d, 5.3)	30.8	3.03 (t, 8.3)
10'	19.3	1.20 (d, 5.3)	7.5	2.09 (s)
11'	7.5	2.11 (s)		
1''			141.6	
2'', 6''			125.9 ^a	7.19-7.31 (overlapped) ^a
3'', 4'', 5''			128.5 ^a	7.19-7.31 (overlapped) ^a
3 -OCH ₃	61.9	3.88 (s)	62.0	3.87 (s)
5 -OH		9.69 (s)		9.60 (s)
1'-OH		11.33 (s)		11.33 (s)
3'-OH		12.39 (s)		12.41 (s)
5'-OH		10.50 (s)		10.41 (s)

^a Overlapping resonances within the same column

2.3.3. Structure of baeckenones D (**4**) and E (**5**)

Compound **4** was a colorless needles. The molecular formula of **4** was determined by HREIMS to be $C_{15}H_{22}O_5$, by the ion peak at m/z 282.1477 $[M]^+$. The IR spectrum displayed absorption bands of a hydroxyl group (3395 cm^{-1}) and a conjugated carbonyl group (1604 cm^{-1}). The ^1H NMR spectra of **4** (Table 2.3, Figure 2.10) revealed signals for an olefinic methine proton [δ_{H} 6.94 (s)], an aryl methyl group [δ_{H} 1.90 (s)], a methoxy proton [δ_{H} 3.92 (s)], three singlets of tertiary methyl groups [δ_{H} 1.42 (s), 1.35 (s), 1.17 (s)], a methylene proton [δ_{H} 1.69 (2H, q, $J = 7.6$ Hz)], a triplet of a terminal methyl group [δ_{H} 0.95 (t, $J = 7.6$ Hz)], and a hydroxy proton [δ_{H} 3.24 (s)]. The ^{13}C NMR spectrum (Table 2.3) showed the presence of five methyl groups (δ_{C} 24.9, 21.6, 16.5, 10.1, and 7.8), a methoxy carbon (δ_{C} 61.9), a methylene carbon (δ_{C} 30.5), an olefinic methine carbon (δ_{C} 139.1), a carbonyl carbon (δ_{C} 186.1), a hemiacetal carbon (δ_{C} 98.5), an aliphatic quaternary carbon (δ_{C} 45.8), an oxygenated quaternary carbon (δ_{C} 81.4), two olefinic quaternary carbons (δ_{C} 133.0, 117.4), and an oxygenated olefinic quaternary carbon (δ_{C} 178.2). The 1D NMR data of **4** closely resembled those of the unusual *endoperoxide* phloroglucinol (**14**), isolated in this study. However, the significant differences were the absence of a methyl group and the presence of an ethyl group at C-8 in **4**, as confirmed by the ^1H - ^1H COSY correlation between H₂-10 (δ_{H} 1.69) and δ_{H} H₃-11 (δ_{H} 0.95), as well as the HMBC correlations of H₂-10 and δ_{H} H₃-11 to the oxygenated quaternary carbon (δ_{C} 81.4, C-8) (Figure 2.12). In the HMBC spectrum of **4**, the correlations of H₃-12 (δ_{H} 1.90) to C-1 (δ_{C} 186.1), C-2 (δ_{C} 117.4), and C-3 (δ_{C} 178.2), of the methoxy group (δ_{H} 3.92) to C-3, and of H₃-13 (δ_{H} 1.35) and H₃-14 (δ_{H} 1.17) to C-3 and C-4 (δ_{H} 45.8) confirmed the positions of the aryl

methyl group (H₃-12) at C-2, the methoxy group at C-3, and the *gem*-dimethyl groups at C-4, respectively. Furthermore, the HMBC correlations of H-7 (δ_{H} 6.94) to C-1 and C-5 (δ_{C} 98.5), of H₃-12 to C-1, and of H₃-13 and H₃-14 to C-5 indicated the presence of a phloroglucinol skeleton, and the carbonyl and hydroxyl groups were located at C-1 and C-5, respectively. The connectivity between C-6 in the phloroglucinol unit and the isopentyl unit was deduced from the HMBC correlations of H₃-9 (δ_{H} 1.42) to C-7 (δ_{C} 139.1) and C-8, and of H-7 to C-6 (δ_{C} 133.0) and C-8. The optical rotation value of $[\alpha]_{\text{D}}^{25}$ 0 (c 0.1, CHCl₃) of **4** indicated that compound **4** is a racemic mixture. The relative stereochemistry of **4** was determined on the basis of the NOESY experiment. The NOE correlations between 5-OH and H₂-10, and between H₃-13 and 5-OH, as well as the lack of the correlation between 5-OH and H₃-9, suggested the same orientation among 5-OH, the ethyl group at C-8, and H₃-13 (Figure 2.13). Furthermore, the X-ray crystallographic analysis of **4** supported the relative stereochemistry of **4** (Figure 2.14). Thus, compound **4** was elucidated to be the new, unusual *endoperoxide* phloroglucinol, and was given the trivial name baeckenone D.

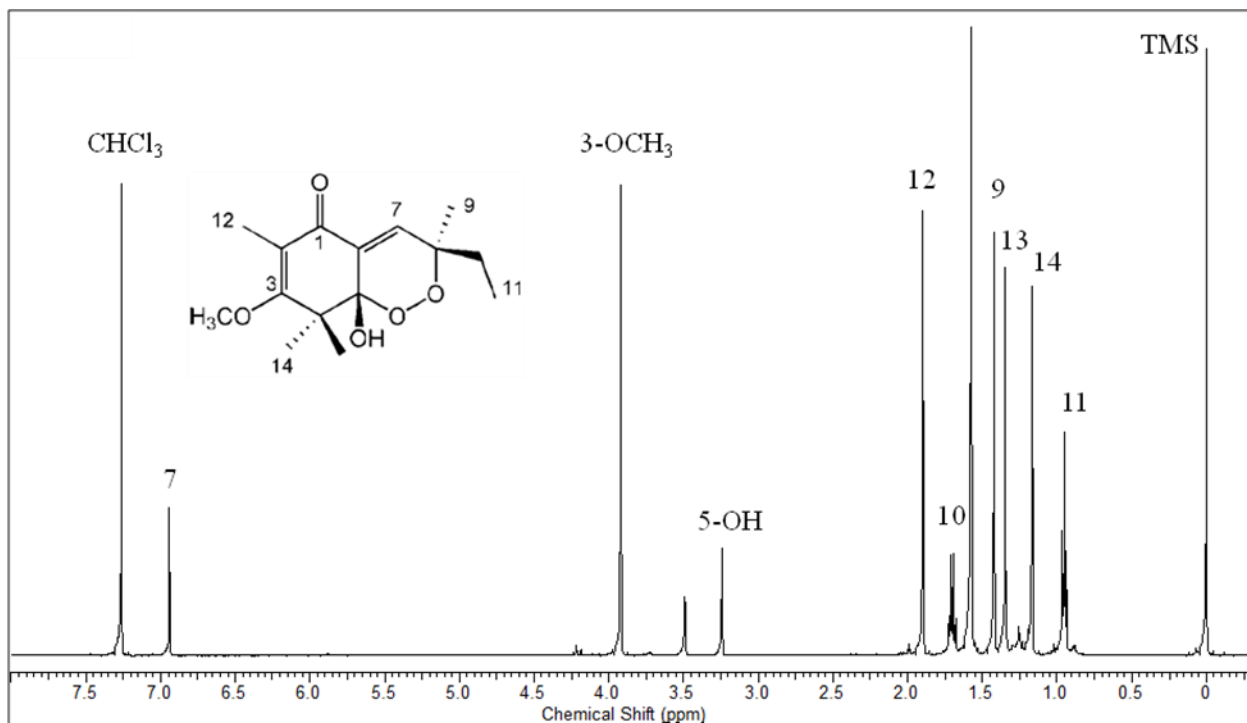


Figure 2.10. ^1H NMR spectrum of **4** in CDCl_3

Compound **5** was obtained as a white powder. The EIMS of **5** showed a molecular ion peak at m/z 282 $[\text{M}]^+$, and its molecular formula was determined to be $\text{C}_{15}\text{H}_{22}\text{O}_5$, by the HREIMS analysis. These data were completely identical to those of **4**. Moreover, the IR, UV, ^1H and ^{13}C NMR data of **5** were quite similar to those of **4** (Table 2.3, Figure 2.11). The detailed analysis of the 2D NMR spectra of **5** confirmed that the planar structure of **5** was the same as that of **4** (Figure 2.12). In contrast, the NOESY correlations between 5-OH (δ_{H} 3.33) and H_3 -9 (δ_{H} 1.34) indicated the same orientation of both the hydroxyl group (5-OH) and the methyl group (H_3 -9), as shown in Figure 2.13. The above evidence indicated that compound **5** was a structural diastereomer of **4**, and was named baeckenone E.

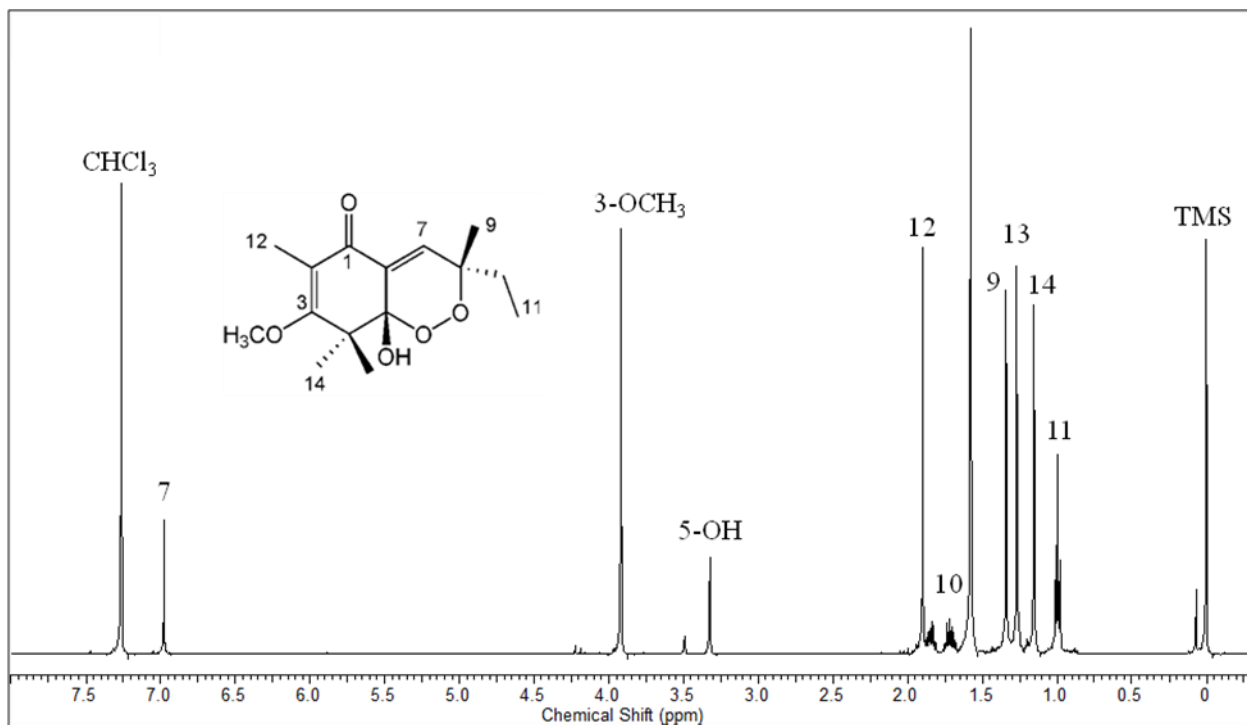


Figure 2.11. ^1H NMR spectrum of **5** in CDCl_3

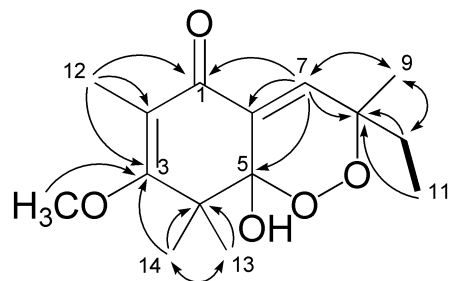


Figure 2.12. Key HMBC (arrows) and ^1H - ^1H COSY (bold lines) correlations of **4** and **5**

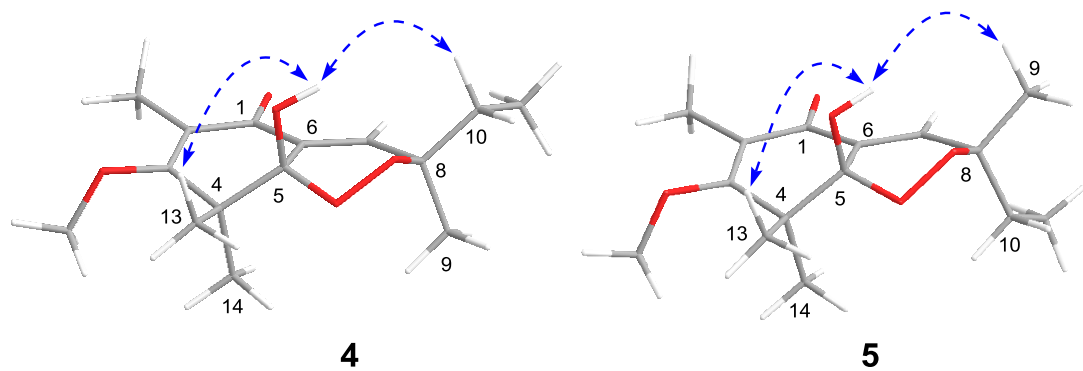


Figure 2.13. Key NOESY correlations of **4** and **5**

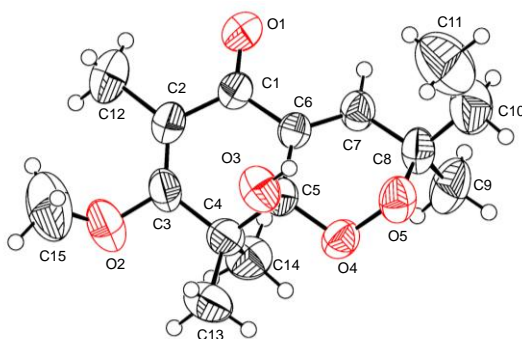


Figure 2.14. ORTEP drawing of the X-ray crystal structure of **4**

Table 2.3. ^1H (600 MHz) and ^{13}C (150 MHz) NMR data for **4** and **5** in CDCl_3

Position	4		5	
	δ_{C}	δ_{H} (mult., J in Hz)	δ_{C}	δ_{H} (mult., J in Hz)
1	186.1		186.4	
2	117.4		117.6	
3	178.2		178.4	
4	45.8		46.0	
5	98.5		98.6	
6	133.0		132.6	
7	139.1	6.94 (s)	139.8	6.98 (s)
8	81.4		81.5	
9	21.6	1.42 (s)	20.3	1.34 (s)
10	30.5	1.69 (q, 7.6)	29.3	1.72 (q, 7.6)
11	7.8	0.95 (t, 7.6)	8.1	0.99 (t, 7.6)
12	10.1	1.90 (s)	10.3	1.90 (m)
13	16.5	1.35 (s)	16.7	1.27 (s)
14	24.9	1.17 (s)	25.1	1.15 (s)
3-OCH ₃	61.9	3.92 (s)	62.1	3.92 (s)
5-OH		3.24 (s)		3.33 (s)

A number of plant species derives a wide variety of phloroglucinols. In the biosynthesis of phloroglucinol, some modifications such as oxidation, prenylation, and C-methylation are occurred to generate a variety of plant-producing phloroglucinols after the skeleton is generated by Type III polyketide synthase (PKS), from condensation of acyl-CoA with malonyl-CoAs through the Claisen-type cyclization. On the basis of the phloroglucinol biosynthetic pathway, phloroglucinol intermediate (i) is proposed to be the precursor of **4** and **5**. Thus, after the α,β -unsaturated carbonyl intermediate (i) was converted into a diene intermediate by the keto-enol tautomerization, the diene intermediate (iia) was cyclized by the singlet oxygen ($^1\text{O}_2$)-involving Diels-Alder type reaction to form **4**. In contrast, the cyclization reaction could be occurred for the intermediate (iib) to produce **5** (Figure 2.15).

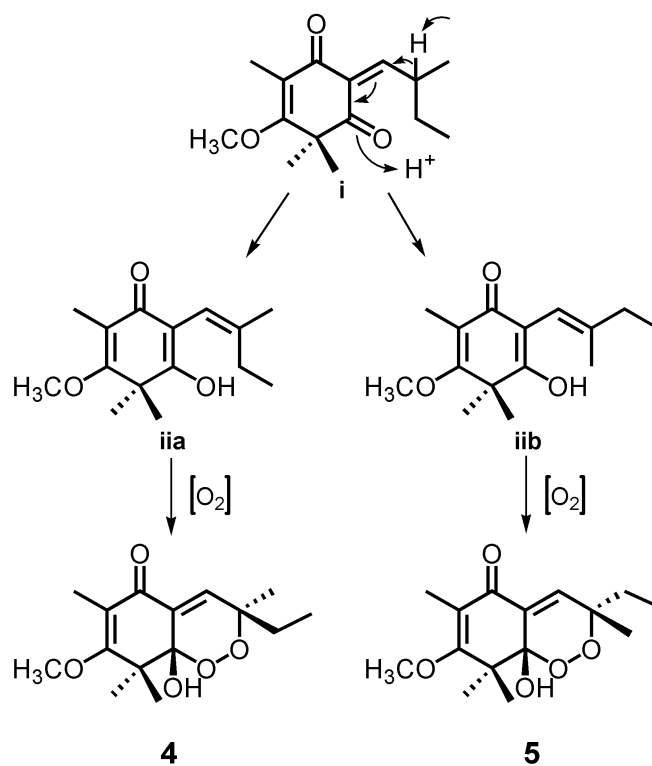


Figure 2.15. Proposed racemization formation of **4** and **5**

2.3.4. Structure of baeckenone F (**6**)

Compound **6** was obtained as a yellow amorphous powder. The HREIMS analysis of **6** showed a molecular ion peak at m/z 254.1528 $[M]^+$, consistent with the molecular formula of $C_{14}H_{22}O_4$. The IR spectrum revealed the presence of a hydroxyl group at 3444 cm^{-1} and a conjugated carbonyl at 1668 cm^{-1} . The ^1H NMR data of **6** (Table 2.4) indicated signals for an oxygenated methine proton [δ_{H} 3.63 (s)], an olefinic methine proton [δ_{H} 5.33 (s)], a methoxy proton [δ_{H} 3.91 (s)], and five tertiary methyl protons with singlets [δ_{H} 1.90 (s), 1.73 (s), 1.71 (s), 1.28 (s), and 1.25 (s)]. The ^{13}C NMR spectrum (Table 2.4) also indicated signals for five methyl carbons (δ_{C} 28.2, 26.9, 19.3, 18.9, and 10.7), a methoxy carbon (δ_{C} 62.1), an sp^2 methine carbon (δ_{C} 121.2), two sp^3 oxygenated methine carbons (δ_{C} 79.6 and 78.7), a carbonyl carbon (δ_{C} 201.1), three sp^2 quaternary carbons (δ_{C} 179.6, 138.2, and 114.4), and an sp^3 quaternary carbon (δ_{C} 43.1). All protons and carbons were assigned by analyzing the 1D NMR, NOESY, HMQC, and HMBC spectra. The presence of a phloroglucinol moiety was verified by the HMBC correlations of H_3 -11 (δ_{H} 1.90) to C-1 (δ_{C} 201.1), C-2 (δ_{C} 114.4), and C-3 (δ_{C} 179.6), of H_3 -12 (δ_{H} 1.25) and H_3 -13 (δ_{H} 1.28) to C-3, C-4 (δ_{C} 43.1), and C-5 (δ_{C} 79.6), and of H-5 (δ_{H} 3.63) to C-4, C-6 (δ_{C} 78.7), C-12 (δ_{C} 18.9), and C-13 (δ_{C} 26.9). In the HMBC spectrum, the methoxy proton at δ_{H} 3.91 was correlated to C-3, suggesting the location of the methoxy group at C-3 in the phloroglucinol moiety. Furthermore, the HMBC correlations of H-7 (δ_{H} 5.33) to C-9 (δ_{H} 19.3) and C-10 (δ_{H} 28.2), and of H_3 -9 (1.71) and H_3 -10 (δ_{H} 1.73) to C-7 (δ_{C} 121.2) and C-8 (δ_{C} 138.2) suggested the existence of an isobutene unit. The attachment between C-7 in the isobutene unit and C-6 in the phloroglucinol unit was deduced, on the basis of the HMBC

correlations of H-7 to C-1 and C-6, and of H-5 to C-6 and C-7. The NOESY experiment of **6** revealed correlations between the protons at H-5 and H-7, which indicated the presence of *syn*-5,6-dihydroxy groups (Figure 2.18). Hence, the relative structure of **6** was identified as shown, and the compound was named baeckenone F.

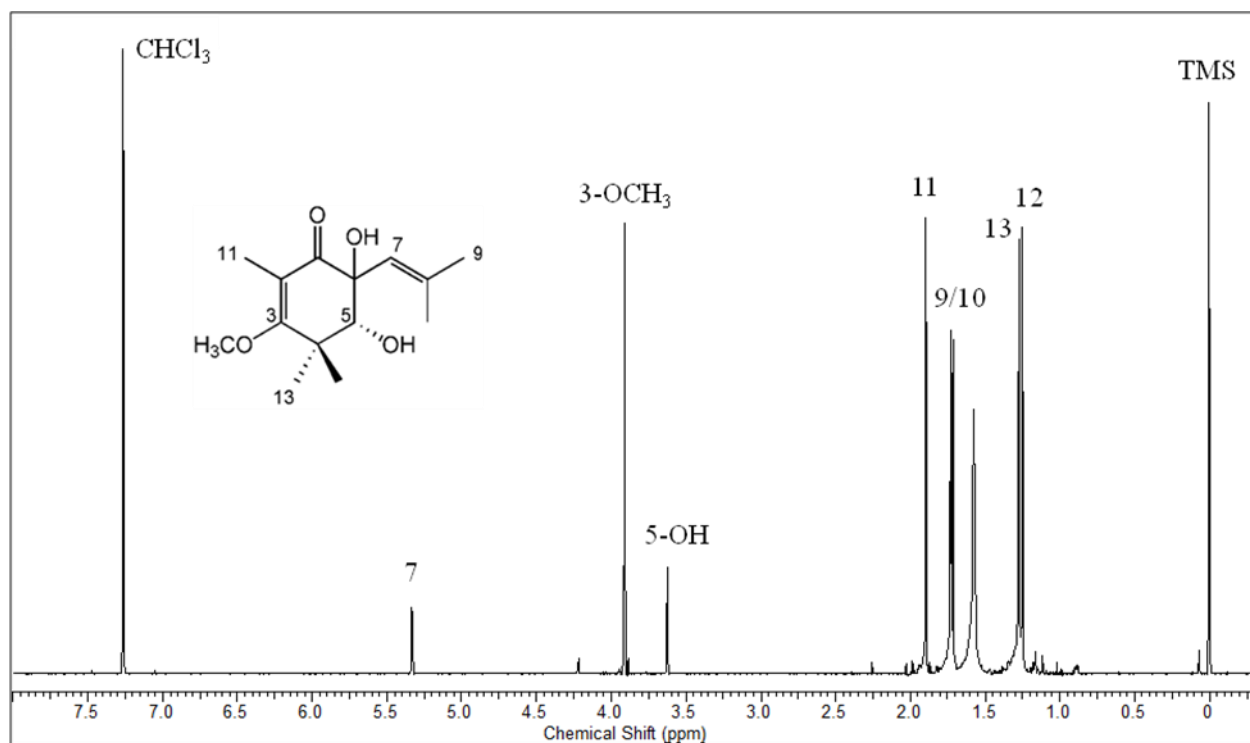


Figure 2.16. ^1H NMR spectrum of **6** in CDCl_3

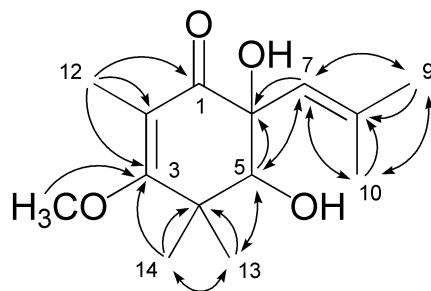


Figure 2.17. Key HMBC (arrows) correlations of **6**

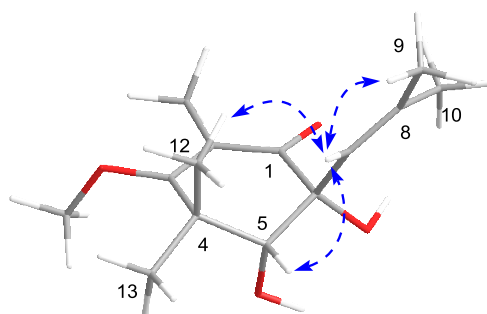


Figure 2.18. NOESY correlations of **6**

Table 2.4. ^1H (600 MHz) and ^{13}C (150 MHz) NMR data for **6** in CDCl_3

Position	6	
	δ_{C}	δ_{H} (mult., J in Hz)
1	201.1	
2	114.4	
3	179.6	
4	43.1	
5	79.6	3.63 (s)
6	78.7	
7	121.2	5.33 (s)
8	138.2	
9	19.3	1.71 (s)
10	28.2	1.73 (s)
11	10.7	1.90 (s)
12	18.9	1.25 (s)
13	26.9	1.28 (s)
14		
3-OCH ₃	62.1	3.91 (s)
5-OH		

2.3.5. Structure of frutescencenones A (**7**) and B (**8**)

Compound **7** was isolated as a pale yellow amorphous powder with the molecular formula $C_9H_{14}O_3$ deduced from its HREIMS data. The IR spectrum showed a characteristic absorption band of an ester group at 1740 cm^{-1} . The ^1H NMR spectral data of **7** (Table 2.5) displayed a methoxy group signal at δ_{H} 4.12 (3H, s, 3-OCH₃), a methyl ester proton appeared at δ_{H} 3.58 (3H, s, 1'-OCH₃), an aryl methyl proton resonating at δ_{H} 1.83 (3H, s), two tertiary methyls groups with singlets [δ_{H} 1.04 (3H, s), 0.96 (3H, s)], and a hydroxyl proton at δ_{H} 6.12 (1H, s, 1-OH). The ^{13}C NMR spectrum confirmed the presence of the methyl ester (δ_{C} 52.4, 1'-OCH₃), and also showed signals of three methyl groups (δ_{C} 24.9, 20.6, 8.4), a methoxy (δ_{C} 60.3), and a hydroxyl substituted carbon (δ_{C} 84.3), and a ketone carbonyl carbon (δ_{C} 200.8), an ester carbonyl carbon (δ_{C} 172.3), an oxygenated olefinic quaternary carbon (δ_{C} 186.8), an olefinic quaternary carbon (δ_{C} 108.7), and an allylic quaternary carbon (δ_{C} 47.6). All proton and carbon signals were accurately assigned by the 2D NMR experiment, including HMQC and HMBC (Figure 2.21). The HMBC correlations of 1-OH (δ_{H} 6.12) to C-1 (δ_{C} 84.3), C-2 (δ_{C} 47.6), and C-5 (δ_{C} 200.8) allowed us to locate the oxygenated quaternary carbon at C-1, between the carbonyl carbon at C-5 and the quaternary carbon at C-2. In addition, the HMBC correlations of the methoxy proton (δ_{H} 3.58) and 1-OH to the ester carbonyl carbon (δ_{C} 172.3) suggested the existence of the methyl ester group at C-1. Moreover, the HMBC correlations of H₃-8 (δ_{H} 1.83) to C-3 (δ_{C} 186.8), C-4 (δ_{C} 108.7), and C-5, of 3-OCH₃ (δ_{H} 4.12) to C-3, and of H₃-6 (δ_{H} 1.04) and H₃-7 (δ_{H} 0.96) to C-1, C-2, and C-3 confirmed the presence of the cyclopent-2-en-1-one skeleton, and the positions of the *gem*-dimethyl groups (C-6/C-7), the

methoxy group (3-OCH₃), and the methyl group (C-8) at C-2, C-3, and C-4, respectively. The NOESY correlations between 1-OH and H₃-6 and between the methoxy group at δ_H 3.58 and H₃-7 indicated the same orientation of 1-OH and H₃-6, as illustrated in Figure 2.22. Consequently, compound **7** was elucidated to be methyl-1-hydroxy-3-methoxy-2,2,4-trimethyl-5-oxocyclopent-3-ene-1-carboxylate, and was given the trivial name frutescencenone A.

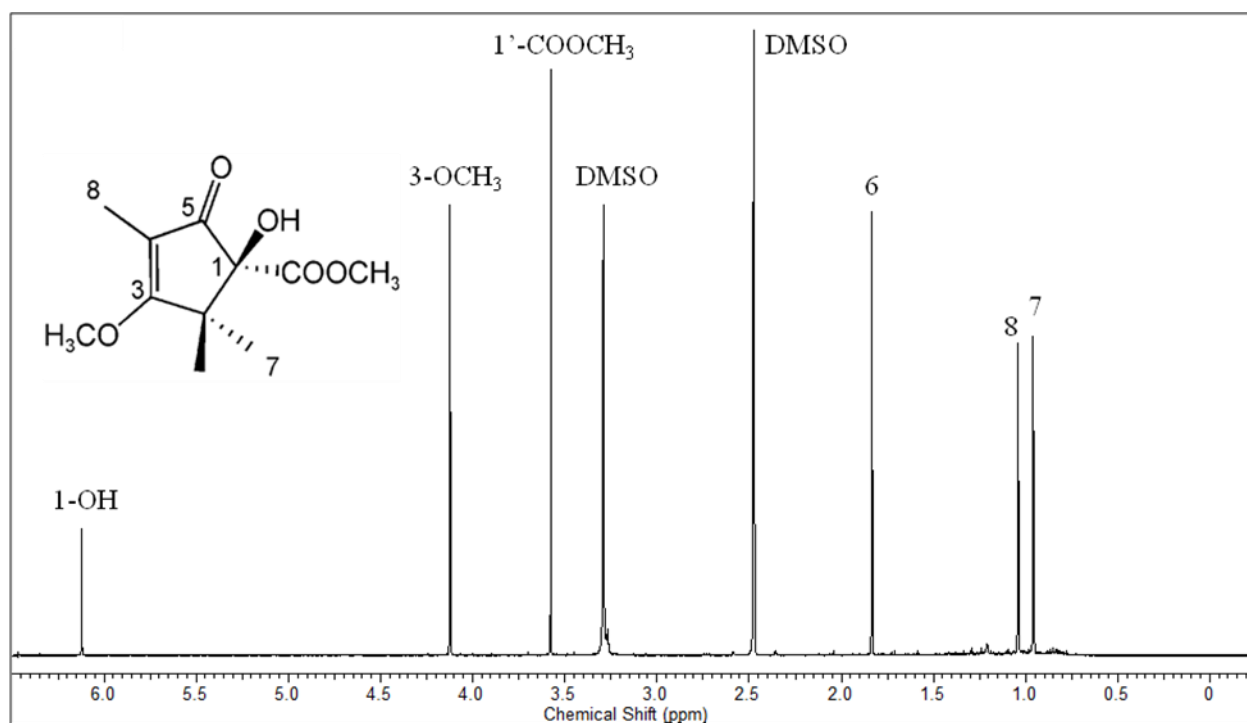


Figure 2.19 ¹H NMR spectrum of **7** in CDCl₃

Compound **8** was isolated as a pale yellow amorphous powder. The molecular formula of **8** was determined to be C₉H₁₄O₃ based on its molecular ion peak at m/z 170.1528 [M]⁺ in the HREIMS. Its spectroscopic data revealed a substructure similar to **7**. The IR spectrum showed the absorption band of hydroxyl and conjugated carbonyl groups at 3421 and 1607 cm⁻¹, respectively. The ¹H NMR spectral data of **8** (Table 2.5) exhibited a methoxy proton at δ_{H} 4.15 (3H, s, 3-OMe), an oxygenated methine proton (δ_{H} 3.90, s), an olefinic methyl proton (δ_{H} 1.94, s), and two methyl groups with singlets [(δ_{H} 1.10, s) and (δ_{H} 1.26, s)]. The ¹³C NMR spectrum also indicated the presence of three methyl groups (δ_{C} 23.7, 22.2, 8.1), a methoxy group (δ_{C} 59.5, 3-OCH₃), an sp³ oxygenated methine carbon (δ_{C} 79.6), a carbonyl carbon (δ_{C} 205.6), an oxygenated olefinic carbon (δ_{C} 187.0), an olefinic quaternary carbon (δ_{C} 107.4), and an aliphatic quaternary carbon (δ_{C} 44.9). The ¹H and ¹³C NMR spectroscopic data of **8** were similar to those of **7**. The difference in **8** was the absence of the methyl ester unit attached to C-1 in **7**. In order to assign all proton and carbon signals accurately, the 2D NMR spectra were measured. The HMBC (Figure 2.21) correlations of H-5 (δ_{H} 3.90) to C-1, C-2, and C-4 confirmed that the oxygenated methine (C-5) was located between the carbonyl group (C-1) and the quaternary carbon (C-4). Furthermore, the position of methoxy group at C-3 was deduced from the HMBC correlation of methoxy proton (δ_{H} 4.15) to C-3 (δ_{C} 187.3). These evidence suggested that the planar structure of **8** was 5-hydroxy-3-methoxy-2,4,4-trimethylcyclopent-2-en-1-one. The NOESY correlations between H-1 and H₃-7 suggested that the oxygenated methine proton and the methyl group are in the same orientation, as shown in Figure 2.22. Hence, the structure of **8** was elucidated, and the compound was named frutescenenone B.

I proposed that **7** and **8** could be derived from baecenone A (**1**). After converted via keto-enol tautomerization of **1**, the enol derivative would be oxidized by oxygenase to form an epoxide intermediate, which is further converted into a cyclopentenone aldehyde via a C-C bond cleavage and a rearrangement. Then, the cyclopentenone aldehyde is converted into carboxylic acid and finally, an esterification of carboxylic acid would produce **7**, while a decarboxylation of carboxylic acid might form **8**. (Figure 2.23).

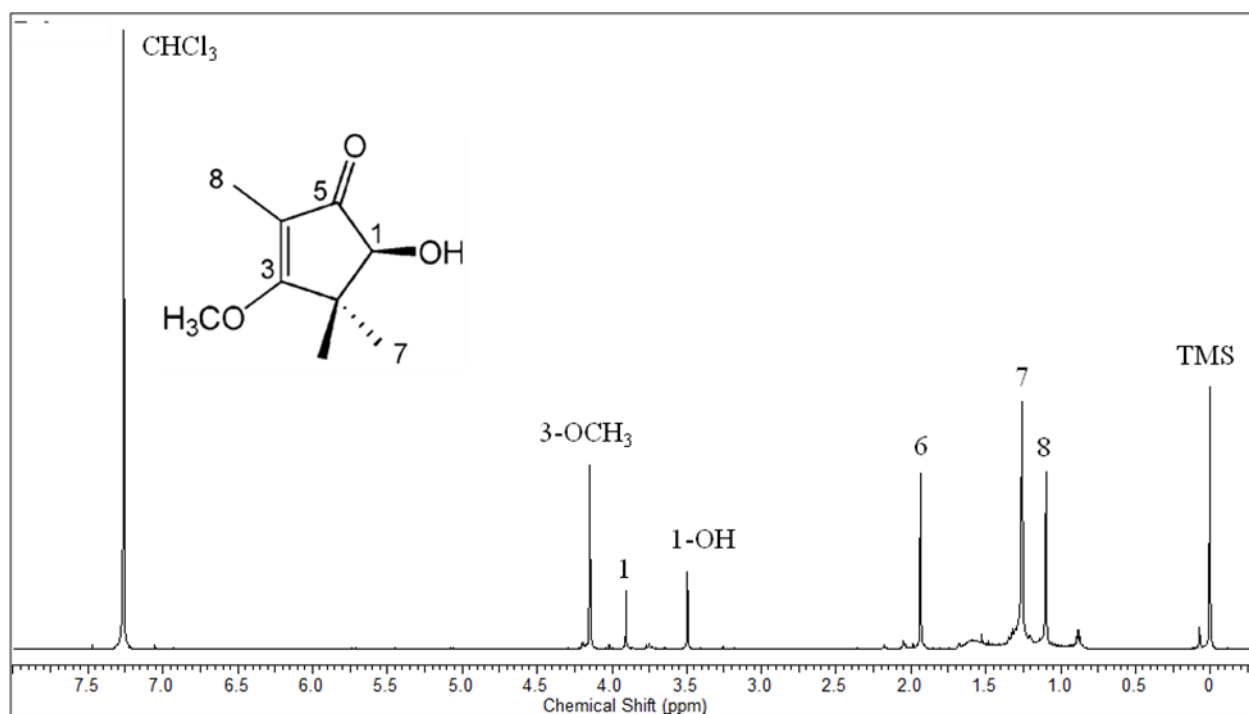


Figure 2.20. ¹H NMR spectrum of **8** in CDCl₃

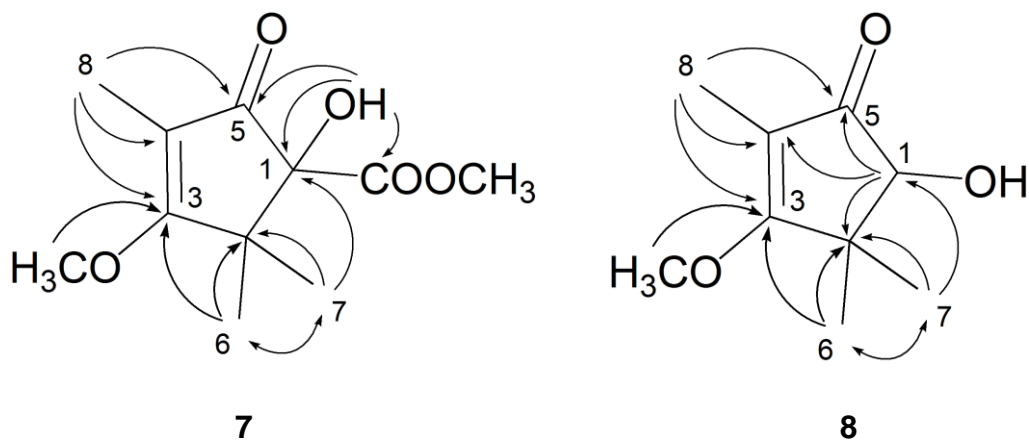


Figure 2.21. Key HMBC correlations (arrows) of **7** and **8**

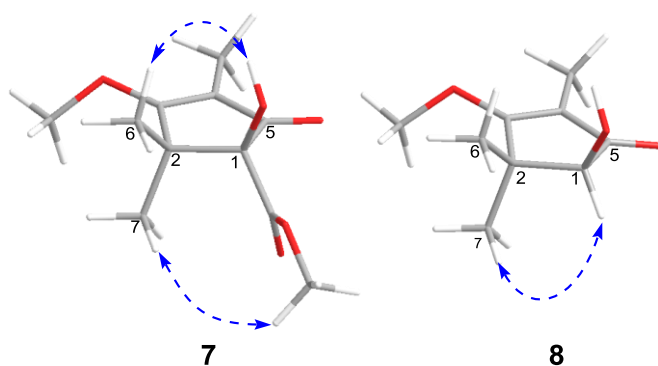


Figure 2.22. Key NOESY correlations of **7** and **8**

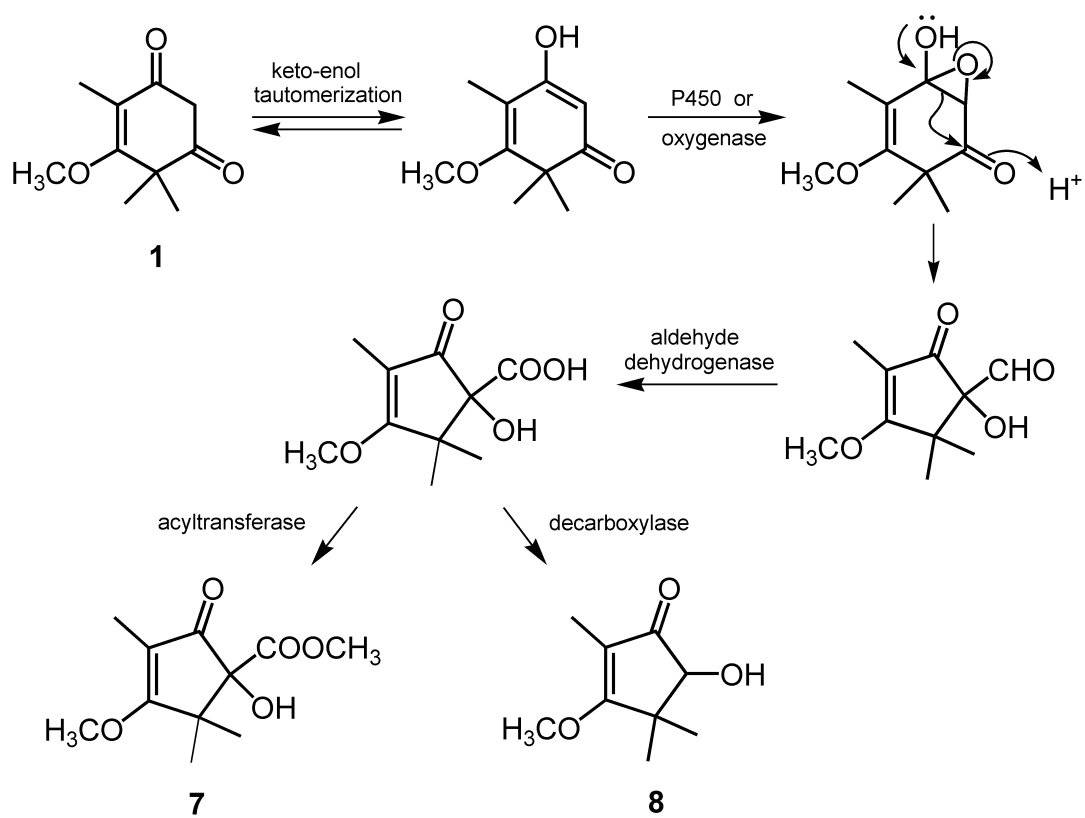


Figure 2.23. Proposed biosynthetic pathway of **7** and **8**

Table 2.5. ^1H (600 MHz) and ^{13}C (150 MHz) NMR data for **7** and **8**

Position	7 in $\text{DMSO-}d_6$		8 in CDCl_3	
	δ_{C}	δ_{H} (mult., J in Hz)	δ_{C}	δ_{H} (mult., J in Hz)
1	84.3		79.6	3.90 (s)
2	47.6		44.9	
3	186.8		187.0	
4	108.7		107.4	
5	200.8		205.6	
6	24.9	1.04 (s)	22.2	1.10 (s)
7	20.6	0.96 (s)	23.7	1.25 (s)
8	8.4	1.83 (s)	8.1	1.93 (s)
COOCH_3	172.3			
3- OCH_3	60.3	4.12 (s)	59.5	4.15 (s)
COOCH_3	52.4	3.58 (s)		
5-OH		6.12 (s)		3.50 (s)

2.3.6. Structure of frutescencenone C (**9**)

Compound **9** was obtained as a pale yellow amorphous powder. The EIMS of **9** exhibited a molecular ion peak at m/z 236 $[M]^+$. Its molecular formula was established as $C_{13}H_{16}O_4$, from the HREIMS and ^{13}C NMR data. The IR spectrum of **9** indicated strong absorption bands of γ -lactone and α,β -unsaturated carbonyl groups at 1752 and 1699 cm^{-1} , respectively. The 1H NMR spectra of **9** (Table 2.6) revealed proton signals for an olefinic methine proton [δ_H 7.85 (1H, s), an allylic methyl group at δ_H 1.96 (s)], and two *gem*-dimethyl groups with singlets [δ_H 1.58 (6H, s, overlapped), 1.39 (6H, s, overlapped)]. The ^{13}C NMR spectrum displayed 13 carbon signals, including five methyl groups (δ_C 25.7, C-6'/C-7' overlapped; 23.3, C-7/C-8 overlapped, and 6.92; C-6), an olefinic methine carbon (δ_C 162.0), a lactone carbonyl carbon (δ_C 167.8), a carbonyl carbon (δ_C 208.6), two oxygenated quaternary carbons (δ_C 86.0, 85.3), and three quaternary carbons (δ_C 168.5, 125.1, 112.8). In the HMBC spectrum, the correlations of H₃-7/H₃-8 (δ_H 1.39) to C-4 (δ_C 208.6) and C-5 (δ_C 86.0), and those of H₃-6 (δ_H 1.96) to C-2 (δ_C 168.5), C-3 (δ_C 112.8), and C-4 indicated the presence of the furan-3(2*H*)-one moiety, the methyl (H₃-6) group at C-3, and *gem*-dimethyl groups at C-5. Furthermore, the HMBC correlations of H₃-6'/H₃-7' (δ_H 1.58) to C-4' (δ_C 162.0) and C-5' (δ_C 85.3), and of H-4' (δ_H 7.85) to C-2' (δ_C 167.8), C-3' (δ_C 125.1), and C-5' suggested the existence of a 2(5*H*)-furanone moiety. The connectivity of the two furanone moieties was deduced from the HMBC correlation of H-4' to C-2. Thus, the structure of **9** was established as 3,5,5,5'-pentamethyl-[2,3'-bifuran]-2',4(5*H*,5'*H*)-dione, and it was named frutescencenone C.

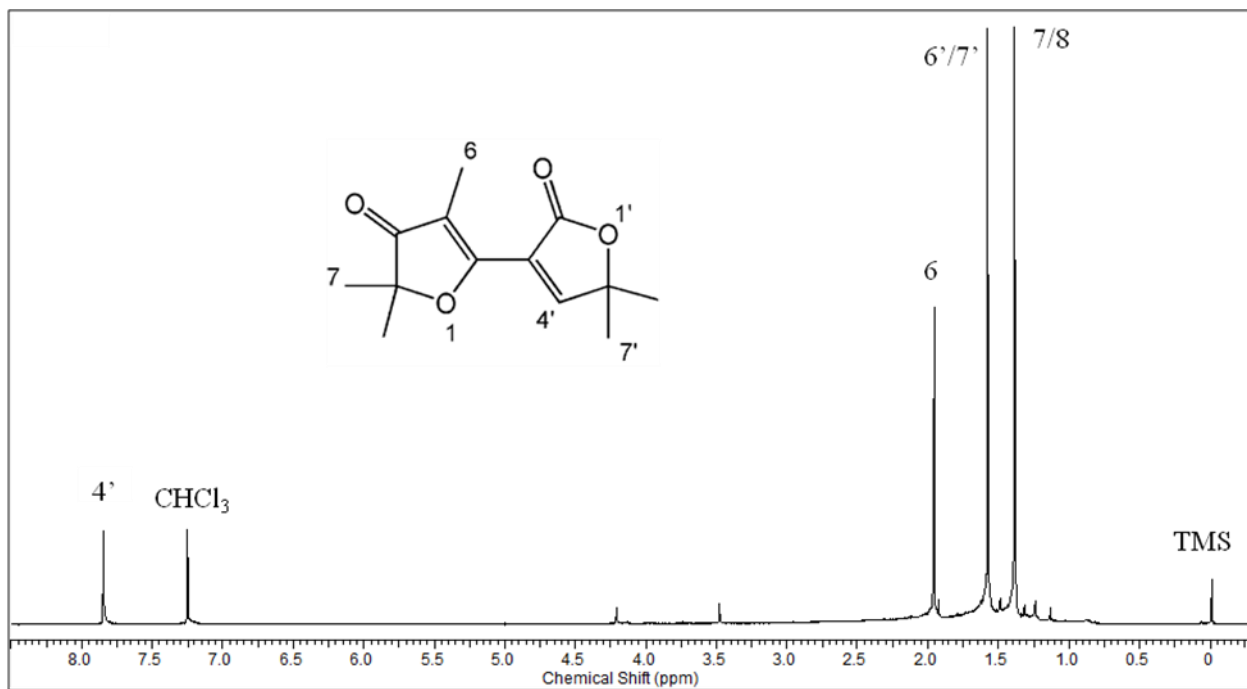


Figure 2.24. ^1H NMR spectrum of **9** in CDCl_3

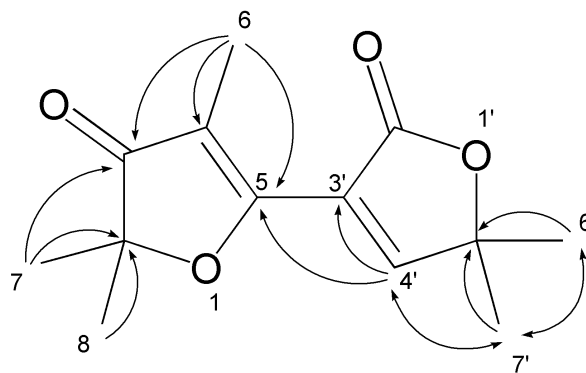


Figure 2.25. Key HMBC correlations (arrows) of **9**

Table 2.6. ^1H (600 MHz) and ^{13}C (150 MHz) NMR data for **9** in CDCl_3

Position	9	
	δ_{C}	δ_{H} (mult., J in Hz)
1		
2	86.0	
3	208.6	
4	112.8	
5	168.5	
6	6.9	1.97 (s)
7,8 ^a	23.3	1.39 (s)
2'	167.8	
3'	125.1	
4'	162.0	7.85 (s)
5'	85.3	
6', 7' ^a	25.7	1.58 (s)

^a Overlapping resonances within the same column

2.3.7. Structure of baeckenones G (**10**) and H (**11**)

Compound **10** was isolated as a pale yellow amorphous powder. The EIMS of **10** revealed a molecular ion peak at m/z 270 $[M]^+$, and its molecular formula was determined to be $C_{13}H_{18}O_6$ by HREIMS in conjunction with NMR analysis. The IR spectrum of **10** displayed strong absorption bands corresponding to conjugated carbonyl (1574 cm^{-1}) and hydroxy groups (3298 cm^{-1}). The ^1H -NMR spectra of **10** (Table 2.7) exhibited signals for an olefinic methine proton [δ_{H} 7.32 (1H, s)], five singlets of tertiary methyl groups [δ_{H} 1.64 (3H, s), 1.52 (3H, s), 1.41 (3H, s), 1.40 (3H, s), 1.04 (3H, s)], and two hydroxyl groups [δ_{H} 3.75 (1H, s), 3.49 (1H, s)]. The careful analyses of the ^{13}C -NMR and HMQC spectra showed the presence of five methyl carbons (δ_{C} 27.5, 24.1, 23.8, 21.3, and 15.5), an olefinic methine carbon (δ_{C} 145.1), an olefinic quaternary carbon (δ_{C} 131.0), two oxygenated quaternary carbons [δ_{C} 79.9 (overlapped)], an acetal carbon (δ_{C} 97.3), an aliphatic quaternary carbon (δ_{C} 52.1), and two ketone carbons (δ_{C} 207.2, 195.6). The assignment of proton and carbon signals was confirmed by the detailed analyses of HMBC and HMQC spectra. The ^1H and ^{13}C NMR spectra were closely similar to those of the known *endoperoxide* phloroglucinol, G-regulator (G-3), isolated from *Eucalyptus grandis*.^{41,44} However, the significant differences were the absence of a methyl group at C-2 in *endoperoxide* G-3 and the presence of a hydroxy group at C-2 in **10**, as deduced from the downfield shift of the oxygenated quaternary carbon at δ_{C} 79.9 (C-2) as well as the HMBC correlations of H₃-11 (δ_{H} 1.64) to C-1 (δ_{C} 95.6), C-3 (δ_{C} 207.2), and C-2. The location of the *gem*-dimethyl groups at C-4 and the hydroxy group at C-5 was confirmed by the HMBC correlations of H₃-12 (δ_{H} 1.04) and H₃-13 (δ_{H} 1.40) to C-3 (δ_{C} 207.2), C-4 (δ_{C} 52.1), and C-5 (δ_{C}

97.3), and of H-7 (δ_{H} 7.32) to C-5. In the NOESY experiments, the NOESY correlation between H₃-13 and 5-OH suggested the same orientation between 5-OH and H₃-13, as illustrated in Figure 2.28. Thus, compound **10** was elucidated to be the new *endoperoxide* phloroglucinol and named as baeckenone G.

I propose that *endoperoxide* (**10**) is generated from a biogenetic precursor, phloroglucinol (i) with a chiral center at C-2 via a biosynthetic route similar to those of **4** and **5** (see Chapter 2.3.2) as follows. (1) The keto-enol tautomerization converts phloroglucinol (i) into a diene intermediate (ii). (2) The singlet oxygen (¹O₂)-involving Diels-Alder type reaction followed by a stereo-control with the methyl or hydroxyl groups at the chiral center (C-2) of the diene intermediate (ii) cyclizes the intermediate (ii) to specifically produce *endoperoxide* (**10**) (Figure 2.29).

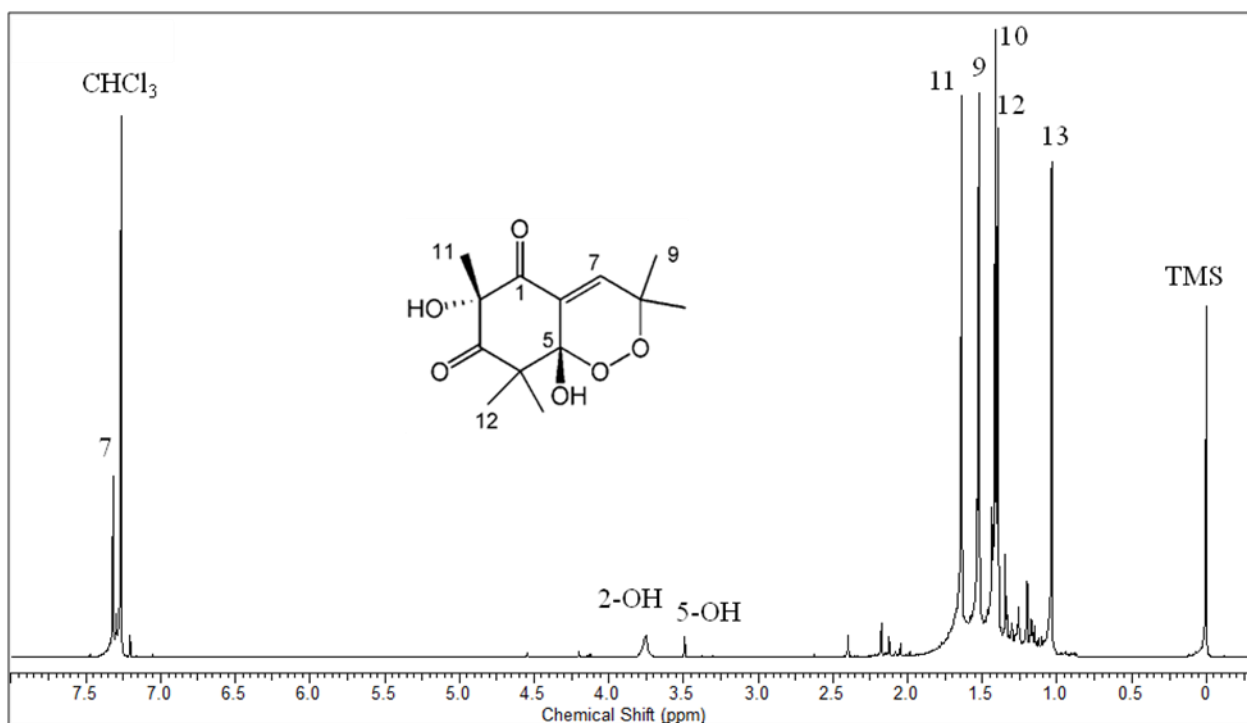


Figure 2.26. ¹H NMR spectrum of **10** in CDCl₃

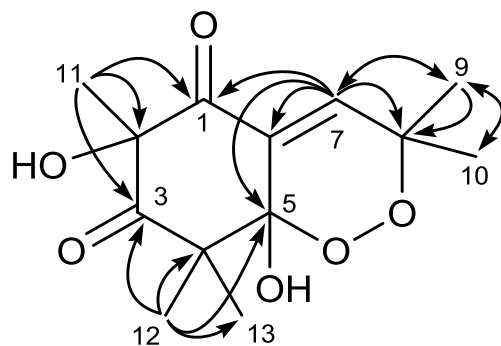


Figure 2.27. Key HMBC (arrows) correlations of **10**

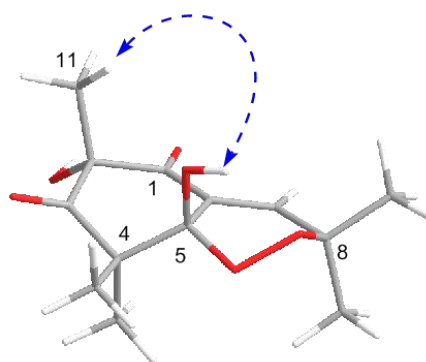


Figure 2.28. Key NOESY correlations of **10**

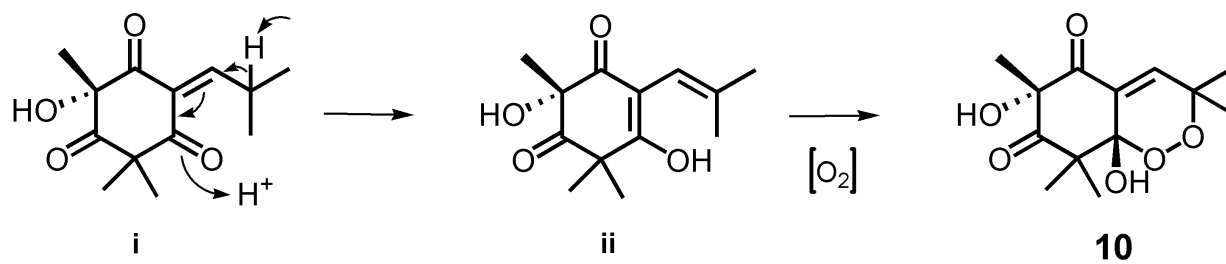


Figure 2.29. Proposed biosynthetic pathway of **10**

Compound **11** was obtained as a pale yellow oil. The HRESIMS of **11** showed a molecular ion peak at m/z 254.1163 $[M]^+$, due to the molecular formula $C_{13}H_{18}O_5$ with three degrees of unsaturation. The IR spectrum peaks at 3445 and 1616 cm^{-1} revealed the presence of a hydroxyl and a conjugated carbonyl groups, respectively. The ^1H NMR data (Table 2.7, Figure 2.30) exhibited four methyl groups [δ_{H} 1.86 (3H, s), 1.58 (3H, s), 1.21 (3H, d, $J = 6.7$ Hz), 1.14 (3H, d, $J = 6.7$ Hz)], a methoxy proton [δ_{H} 4.22 (3H, s)], a aliphatic methine proton [δ_{H} 3.82 (hept)], and two hydroxyl groups [δ_{H} 19.01 (s), 3.90 (s)]. The ^{13}C NMR spectrum (Table 2.7) of **11** revealed thirteen signals including two ketone carbons (δ_{C} 206.9, 196.7), two oxygenated olefinic quaternary carbons (δ_{C} 190.4, 170.2), two olefinic quaternary carbons (δ_{C} 110.2, 103.2), an oxygenated aliphatic quaternary carbon (δ_{C} 76.1), a methoxy carbon (δ_{C} 60.6), an aliphatic methine carbon (δ_{C} 35.1), and four methyl carbons (δ_{C} 29.7, 19.2, 18.7, and 7.9). ^1H - ^1H COSY correlations of H-8 (δ_{H} 3.82) with H₃-9 (δ_{H} 1.21) and H₃-10 (δ_{H} 1.14) as well as the HMBC correlations of H-8 to C-7 (δ_{C} 206.9), and of H₃-9 and H₃-10 to C-8 (δ_{C} 35.1) and C-7 suggested the presence of an isobutyryl unit (Figure 2.31). Furthermore, the existence of cyclohexadiene moiety was confirmed by the HMBC correlations of H₃-11 (δ_{H} 1.58) to C-1 (δ_{C} 196.7), C-2 (δ_{C} 76.1), and C-3 (δ_{C} 170.2), of the methoxy proton (δ_{H} 4.22) to C-3, and of H₃-12 to C-3, C-4 (δ_{C} 110.2), and C-5 (δ_{C} 170.2). These observations also supported that the methyl (H₃-11), the methoxy, the allylic methyl (H₃-12), and the vinyl alcohol located at C-2, C-3, C-4, and C-5, respectively. Thus, compound **11** was elucidated as a new acylphloroglucinol and given trivial name baeckenone H.

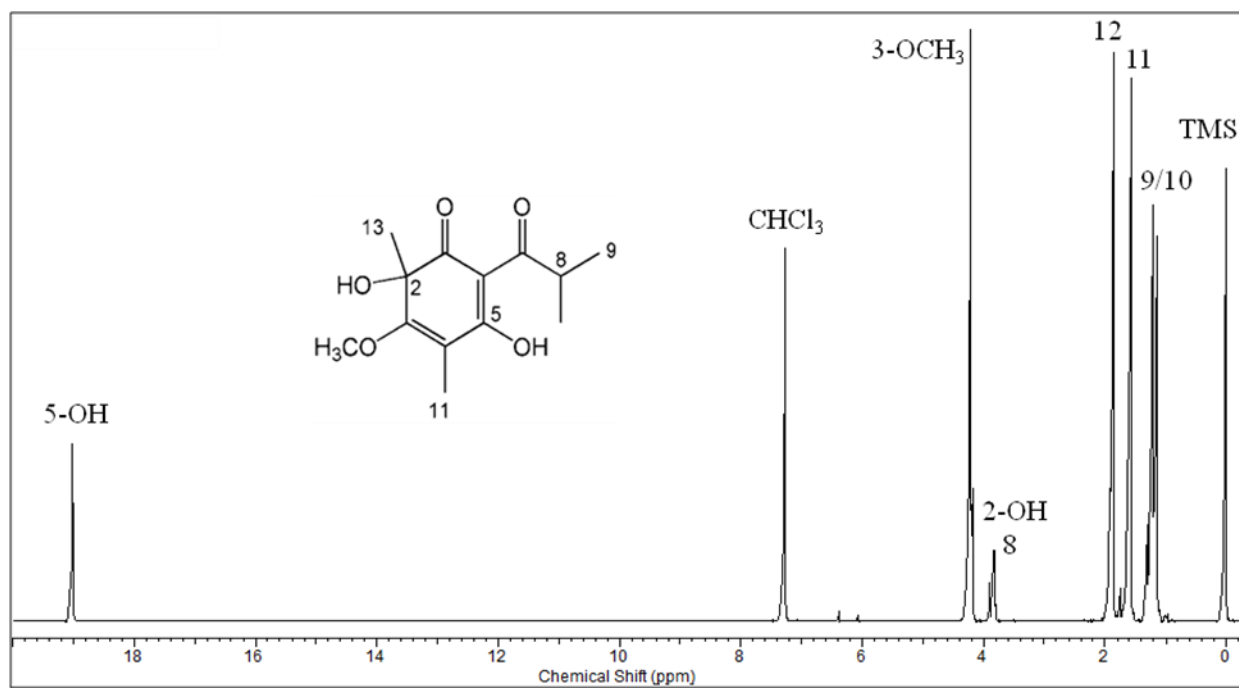


Figure 2.30. ^1H NMR spectrum of **11** in CDCl_3

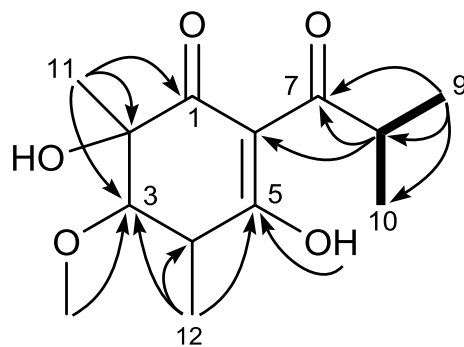


Figure 2.31. Key HMBC (arrows) and ^1H - ^1H COSY (bold lines) correlations of **11**

Table 2.7. ^1H (500 MHz) and ^{13}C (125 MHz) NMR data for **10** and **11** in CDCl_3

Position	10		11	
	δ_{C}	δ_{H} (mult., J in Hz)	δ_{C}	δ_{H} (mult., J in Hz)
1	195.6		196.7	
2	79.9		76.1	
3	207.2		170.2	
4	52.1		110.2	
5	97.3		190.4	
6	131.0		103.2	
7	145.1	7.32 (s)	206.9	
8	79.9		35.1	3.82 (hept, 6.7)
9	27.5	1.52 (s)	19.2	1.21 (d, 6.7)
10	23.8	1.41 (s)	18.7	1.14 (d, 6.7)
11	21.3	1.64 (s)	29.7	1.58 (s)
12	24.1	1.04 (s)	7.9	1.86 (s)
13	15.5	1.40 (s)		
2-OH		3.75 (s)		3.90 (s)
5-OH		3.49 (s)		19.01 (s)
-OCH ₃			60.6	4.22 (s)

2.3.8. Structure of baeckenone I (**12**)

Compound **12** was obtained as a white amorphous powder. The molecular formula was deduced as C₁₅H₂₂O₄ on the basis of its HREIMS peak at m/z 266.1513 [M]⁺. Its IR spectrum showed absorption bands for symmetric (2849 cm⁻¹) and non-symmetric (2916 cm⁻¹) stretching vibration of O-CH₃ group. The ¹H-NMR spectrum of **12** (Table 2.8, Figure 2.32) showed signals for an oxygenated methine proton [δ_{H} 4.29 (s)], two methoxy groups [δ_{H} 3.85 (3H, s), 3.51 (3H, s)], an allylic methyl proton [δ_{H} 1.91 (3H, s)], and four singlets of tertiary methyl groups [δ_{H} 1.48 (3H, s.), 1.38 (3H, s), 1.30 (6H, s, overlapped)]. The ¹³C-NMR spectrum (Table 2.8) displayed 15 signals including two methoxy groups (δ_{C} 61.9, 58.9), a carbonyl carbon (δ_{C} 185.7), two oxygenated olefinic quaternary carbons (δ_{C} 178.7, 171.6), two olefinic quaternary carbons (δ_{C} 119.0, 111.5), an oxygenated aliphatic quaternary carbon (δ_{C} 92.5), an aliphatic quaternary carbon (δ_{C} 40.6), an oxygenated methine carbon (δ_{C} 84.8), an allylic methyl carbon (δ_{C} 9.6), and two sets of *gem*-dimethyl groups. In the HMBC spectrum of **12** (Figure 2.33), the correlations of H-7 (δ_{H} 4.29) to C-5 (δ_{C} 185.7), C-6 (δ_{C} 111.5), and C-8 (δ_{C} 92.5), of H₃-11 (δ_{H} 1.91) to C-1 (δ_{C} 185.7), C-2 (δ_{C} 119.0), and C-3 (δ_{C} 171.6), and of H₃-12 (δ_{H} 1.30) and H₃-13 (δ_{H} 1.38) to C-3, C-4 (δ_{C} 40.6), and C-5 (δ_{C} 178.7) suggested the presence of a dihydrobenzofuran-4(2*H*)-one moiety, and the location of the allylic methyl (H₃-11) and *gem*-dimethyl (H₃-12, H₃-13) groups at C-2 and C-4, respectively. Furthermore, the position of the methoxy (δ_{H} 3.85) at C-3, the methoxy (δ_{H} 3.51) at C-7, and the *gem*-dimethyl (H₃-9, H₃-10) groups were deduced from the HMBC correlations of the methoxy proton at δ_{H} 3.85 to C-3, of the methoxy proton at δ_{H} 3.51 to C-6, of H-7 to the methoxy carbon at δ_{C} 58.9, C-9 (δ_{C} 26.6), and C-10 (δ_{C} 20.4), and of H₃-9 (δ_{H} 1.30) and H₃-10 (δ_{H} 1.48) to C-7 and C-8. The NOESY

correlations between H-7 and H₃-12, and between H₃-12 and H₃-10 suggested the same orientation among H-7, H₃-10, and H₃-12 (Figure 2.34). Finally, the structure of compound **12** was deduced as 3,6-dimethoxy-2,2,5,7,7-pentamethyl-3,7-dihydro-2*H*-benzofuran-4-one and named baeckenone I.

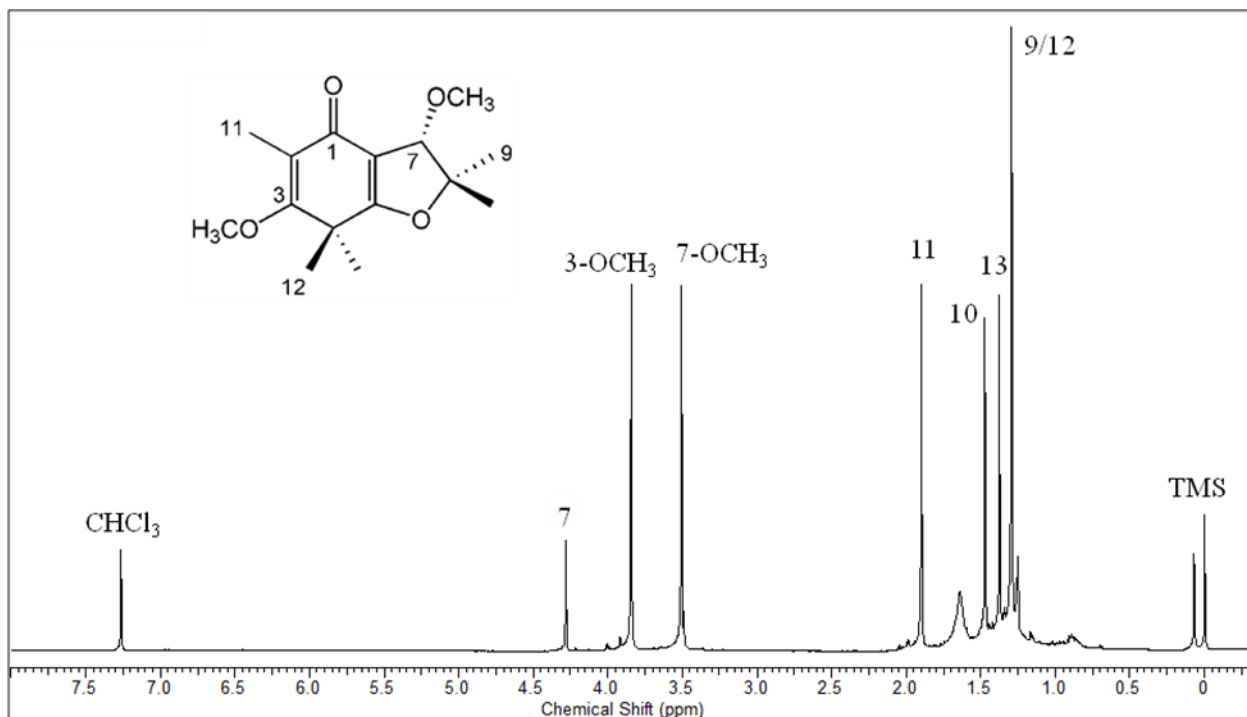


Figure 2.32. ¹H NMR spectrum of **12** in CDCl₃

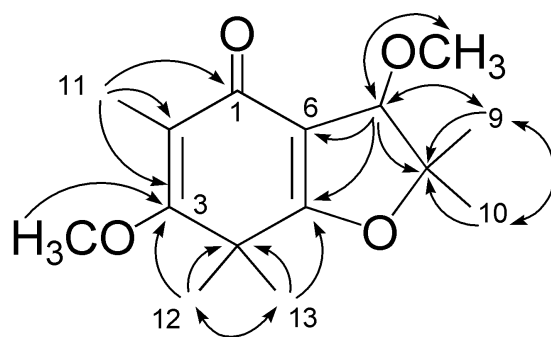


Figure 2.33. Key HMBC correlations (arrows) of **12**

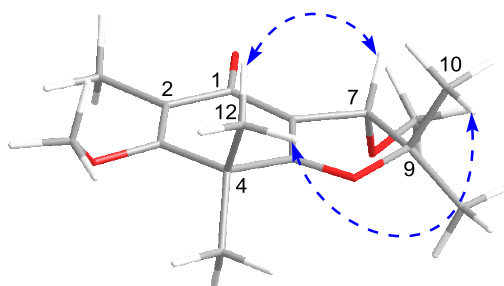


Figure 2.34. Key NOESY correlations (dashed arrows) of **12**

Table 2.8. ^1H (500 MHz) and ^{13}C (125 MHz) NMR data for **12** in CDCl_3

Position	12	
	δ_{C}	δ_{H} (mult., J in Hz)
1	185.7	
2	119.0	
3	171.6	
4	40.6	
5	178.7	
6	111.5	
7	84.8	4.29 (s)
8	92.5	
9	26.6	1.30 (s) ^a
10	20.4	1.48 (s)
11	9.6	1.91 (s)
12	23.4	1.30 (s) ^a
13	22.3	1.38 (s)
3-OCH ₃	61.9	3.85 (s)
7-OCH ₃	58.9	3.51 (s)

^a Overlapping resonances within the same column

2.4. Summary of Chapter 2

Phytochemical investigation of *B. frutescens* leaves led to the isolation of 12 new compounds (**1-12**) and 10 known compounds (**13-22**). To our knowledge, **16** was isolated for the first time as a natural product although its synthesis has been described by Buyk et al.³⁵

Chapter 3 Biological Activities of Constituents Isolated from

Baeckea frutescens

3.1. Introduction

The twenty-two isolated compounds from *B. frutescens* were further assessed for their antibacterial activity against several bacterial strains, according to the method described in the previous section. In addition, cytotoxic activity of the isolated compounds was also evaluated.

3.2. Antibacterial Activities of Compounds Isolated from the leaves of *B. frutescens*

The antibacterial activities of the isolated compounds (**1–22**) against *B. subtilis*, *S. aureus*, *M. smegmatis*, *E. coli*, and *K. pneumoniae* were assessed by using the standard microdilution methods. Ampicillin was used as a positive control. All compounds showed no antibacterial activity against the Gram-negative bacterial strains, *E. coli* and *K. pneumoniae*, and the Gram-negative bacterial strain, *M. smegmatis* at a concentration of 100 μM . However, baeckenone B (**2**) exhibited good inhibitory activities against both *B. subtilis* and *S. aureus* with MIC values of 40 μM and 50 μM , respectively.

Baeckenone B (**2**) is classified as an acylphloroglucinol type of compound. A large number of differently substituted acylphloroglucinol-producing plants have been used in traditional medicine throughout the world and shown to possess various biological activities.⁵⁴ Furthermore, some phloroglucinols from Myrtaceae family exhibited interesting antibacterial activities. For example, grandinol, the monomeric acylphloroglucinol, has been reported to exhibit antibacterial activity against *B. subtilis* with the MIC value of 20 μM .⁴⁴ Moreover eucalyptone isolated from *Eucalyptus globulus* has significant antibacterial activity against *S. mutans* and *S. sobrinus*.⁴⁵ Accordingly, baeckenone B (**2**) may be suggested as a candidate for antibacterial agent.

3.3. Cytotoxic activity of Isolated from the leaves *B. frutescens*

In previous section, a number of phloroglucinol type of compounds has been isolated from *B. frutescens* leaves. The phloroglucinol derivatives reportedly exhibit cytotoxic activities against cancer cell lines such as breast and leukemia cells.²⁴ Therefore, cytotoxic activities of the isolated compounds (**1–22**) were also assessed against human pancreatic (PSN-1), human lung (A549), and breast (MDA-MB231) cancer cell lines. The cytotoxic activity was evaluated by using the standard WST-8 assay method. 5-Fluorouracil was used as a positive control.⁴⁶ Baeckenone F (**6**) showed moderate growth inhibitory activities against three tested cancer cell lines, with half maximal inhibitory concentration (IC_{50}) values ranging from 33.3 μ M to 39.3 μ M. Baeckenone D (**4**) and the known *endoperoxide* phloroglucinol (**14**) exhibited selectively weak growth inhibitory activity against the A549 cancer cell line with IC_{50} values of 60 μ M and 74.1 μ M, respectively. Frutescenenone A (**7**) exhibited significant cytotoxic effects against the three cancer cell lines, human lung A549, pancreatic PSN-1, and breast MDA-MB231, with IC_{50} values of 36.3, 29.3, and 38.2 μ M, respectively. In contrast, a new furanone, frutescenenone C (**9**), showed selective cytotoxic activity against the PSN-1 cell line, with an IC_{50} value of 20.1 μ M (Table 3.1).

Table 3.1 Cytotoxic activity of isolated compounds from *B. frutescens* leaves

Compound	IC ₅₀ (μM)		
	A549	PSN-1	MDA-MB231
Baeckenone D (4)	60.0	> 100	> 100
Baeckenone F (6)	34.0	33.3	39.3
Frutescencenone A (7)	36.3	29.3	38.2
Frutescencenone C (9)	88.0	20.1	> 100
5-FU ^a	1.8	2.4	4.0

^a 5-Fluorouracil (5-FU): Positive control

3.4. Summary of Chapter 3

Of the 22 compounds examined, baeckenone B (**2**) showed the most potent antibacterial activities against Gram-positive bacteria, *B. subtilis* and *S. aureus* with the MIC value of 40 μM and 50 μM, respectively. On the other hand, baeckenone F (**6**) and frutescencenones A and C (**7** and **9**) exhibited growth inhibitory activities against three cancer cell lines (A549, PSN-1, MDA-MB231). Phloroglucinol derivatives are major class of the secondary metabolites that widely occur in the biological system. Mainly, phloroglucinols play an important role in the biological control of many plant growth regulations.⁴⁷ Furthermore, phloroglucinol-type secondary metabolites derived from the plants of the Myrtaceae family reportedly possess a wide range of biological activities, including antibacterial, antifungal, antiplasmodial, antimalarial, antitumor, and immunomodulatory effects.⁴⁸⁻⁵³ Further investigation of phloroglucinols in this study may show the other biological activities.

Conclusions

The preliminary study on antibacterial activity of Indonesian medicinal plants was conducted. *B. frutescens* leaves showed significant antibacterial activities against Gram-positive bacteria, *S. aureus* and *B. subtilis* with the MIC values of 100 µg/mL and 200 µg/mL, respectively, while *C. mangga* rhizomes exhibited antibacterial activities against Gram-positive bacteria, *S. aureus* and *B. subtilis* with the MIC values of 200 µg/mL and 150 µg/mL, respectively.

Furthermore, the phytochemical investigation of the CHCl₃ extract of *B. frutescens* leaves led to the isolation of 12 new compounds including phloroglucinol derivatives (**1-6**, **10-12**), cyclopentenones (**7** and **8**), and furanone (**9**), together with 10 known compounds comprising baeckeol (**13**), peroxide phloroglucinol (**14**), cyclopentenone derivative (**15**), 4-hydroxy-2,2,5-trimethyl-cyclopent-4-ene-1,3-dione (**16**), 5,7-dihydroxy-6,8-dimethylflavanone (**17**), 5,7-dihydroxy-6-methylflavanone (**18**), 5,7-dihydroxy-8-methyl-6-prenylated flavanone (**19**), hybrid phloroglucinol (**20**), humulene diepoxide (**21**), and ursolic acid (**22**). The chemical structure of those compounds was determined on the basis of spectroscopic analyses and comparisons of MS and NMR data with those reported in the literature. Among those compounds, **16** was isolated for the first time as a natural product.

Among twenty two compounds examined, compound **2**, named as baeckenone B, showed the most potent antibacterial activities against Gram-positive bacteria, *B. subtilis* and *S. aureus* with the MIC value of 40 µM and 50 µM, respectively. Baeckenone F (**6**) and frutescenenone A (**7**) exhibited significant growth inhibitory activities against human pancreatic (PSN-1), lung

(A549), and breast (MDA-MB-231) cancer cell lines. In contrast, frutescenenone C (**9**) showed selective cytotoxic activity against PSN-1.

In the present work, the chemical investigation of the leaves of *B. frutescens* resulted in the isolation of dimeric phloroglucinols (**2** and **3**), *endoperoxide* phloroglucinols (**4**, **5**, **10** and **14**) and cyclopentenones (**7** and **8**), some of which possessed biological effects such as antibacterial and cytotoxic activities. Thus, it is presumed that the structures of the metabolites are important for exhibiting their biological activities. Particularly, several peroxide metabolites isolated from higher plants and fungi show a wide range of pharmacological activities such as antitumor, antibacterial, antifungal, and antimalarial activities. For example, artemisinin, the sesquiterpene lactone with peroxide bridge isolated from *Artemisia annua*, has been used for the treatment of malaria infection.⁵⁴ It has been proved that the peroxide bridge in the pharmacophore is essential for the expression of the antimalarial activity. However, *endoperoxide*-containing phloroglucinols are rarely occurred in nature.⁵⁵ The *endoperoxide* phloroglucinols in this study might be expected to possess various biological activities. Furthermore, advanced techniques of extraction and purification from unexploited natural resources could allow us to discover novel bioactive *endoperoxide* derivatives in the future. Thus, the derivatives with peroxide bridge may be promising targets and leads for the new drug development.

Experimental Section

I. General Experimental Procedures

Optical rotations were measured on a JASCO DIP-140 digital polarimeter (Japan Spectroscopic Co, Ltd, Tokyo, Japan). IR spectra were analyzed using a JASCO IR-460 plus spectrophotometer (Japan Spectroscopic Co, Ltd, Tokyo, Japan). NMR spectra were recorded using a JEOL JNM-LA400 spectrometer (^1H NMR: 400 MHz, ^{13}C NMR: 100 MHz), Bruker DMX-500 spectrometer (^1H NMR: 500 MHz, ^{13}C NMR: 125 MHz) and a Varian UNITY 600 spectrometer (^1H NMR: 600 MHz, ^{13}C NMR: 150 MHz) with tetramethylsilane (Pure Chemical Industries, Ltd., Osaka, Japan) as an internal standard. High resolution electron impact mass spectrometry (HREIMS) was performed using a JEOL MStation JMS-700 spectrometer. High resolution electron spray ionization mass spectrometry (HRESIMS) was carried out using a Waters SYNAPT G2-Si HDMS spectrometer (Waters, Milford, MA, USA). MPLC was performed using Buchi Labortechnik AG C-615 chromatographic pump and a Yamazen prep UV 254 UV detector operating at 254 nm. Column chromatography was performed on Sephadex LH-20 (GE Healthcare, Little Chalfont, United Kingdom) or silica gel 60 N (40-50 μm ; Kanto Chemical CO., Inc., Tokyo, Japan) and Cosmosil 75C₁₈-OPN (75-140 μm ; Nacalai Tesque, Inc., Kyoto, Japan). Analytical and preparative TLCs were performed using precoated Merck Kieselgel 60F₂₅₄ and RP-18F₂₅₄ plates (0.25 mm thick for analytical TLC and 0.50 mm thick for preparative TLC, Merck, Darmstadt, Germany). Preparative TLC was performed in vertical type rectangular chambers (Yazawa Scientific Co., Ltd., Tokyo, Japan), under

conditions saturated with the developing solvent. The bacterial strains, *Bacillus subtilis* NBRC 3134, *Staphylococcus aureus* NBRC 15035, *Klebsiella pneumoniae* NBRC 3512, *Mycobacterium smegmatis* NBRC 3082, and *Escherichia coli* NBRC 102203, were obtained from National Institute of Technology and Evaluation (NITE, Tokyo, Japan). The cell lines, PSN-1 (human pancreatic cancer), A549 (human lung cancer), and MDA-MB-231 (human breast cancer), were obtained from RIKEN cell bank (Wako, Japan) and maintained in our laboratory. Cell culture flasks and 96-well plates were purchased from Corning, Inc. (Corning, NY, USA). An SH-1200 microplate reader (Corona Electric Co., Ltd., Hitachinaka, Japan) was used to measure the absorbance of the cells in the cytotoxic activity assay.

II. Experimental Detail of Chapter 1

Preparation of the extracts from Indonesian medicinal plants

Twenty-six medicinal plants were purchased from Pasar Gedhe Market, Solo City, Indonesia. Each part of plants was dried at 50 °C in oven, and then ground into fine powder, which was macerated with CHCl₃. After filtration of the suspension, the CHCl₃-solution was evaporated under reduced pressure to furnish the CHCl₃ extract. The residue was extracted with MeOH to give the MeOH extract.

Antimicrobial assay

Antimicrobial activity was performed using the standard MTT assay according to a published procedure with slight modifications. *B. subtilis* NBRC 3134, *S. aureus* NBRC 15035, *K. pneumoniae* NBRC 3512, *M. smegmatis* NBRC 3082, and *E. coli* NBRC 102203 were used for

this assay. These strains were tested by using microdilution assays. Bacterial strains were inoculated on YP agar plates [1% polypeptone (Nihon Pharmaceutical Co., Ltd., Tokyo, Japan), 0.2% yeast extract (Difco, USA), 0.1% MgSO₄·7H₂O, and 2% agar (Nacalai Tesque Inc., Kyoto, Japan)] and incubated at 30 °C for 12 h. A stock sample solution was prepared in DMSO and further diluted to varying concentrations in 96-well plates (Corning, NY, USA) that contained microbial strains incubated in YP medium for the bacterial strains. The plate was further incubated at 37 °C overnight, and ampicillin (Nacalai Tesque) was used as reference reagent for the bacterial strains. Antimicrobial activity MIC values were visual observed by addition of the 50 µL of the 3-(4,5-dimethylthiazol-2-yl)-2,5-dimethyltetrazolium bromide (MTT, Sigma–Aldrich, USA) solution (0.5 mg/mL isopropyl-HCl) into each well and incubation for 1 h.

III. Experimental Detail of Chapter 2

Plant material

The leaves of *B. frutescens* were purchased from Pasar Gedhe Market, Solo City, Indonesia and authenticated by Saifudin Azis Ph.D, Botanist of the School of Pharmacy, Universitas Muhammadiyah Surakarta, Indonesia. The voucher specimen (28298) is preserved in the Museum of Materia Medica, Analytical Research Center for Ethnomedicines, Institute of Natural Medicine, University of Toyama, Toyama, Japan.

Extraction and isolation procedure

The powdered leaves of *B. frutescens* (425 g) were exhaustively extracted with CHCl_3 (3×1.5 L) in an ultrasonic bath for 90 min at room temperature, and the resulting solution was evaporated under reduced pressure to yield the CHCl_3 extract (41 g). The concentrated extract was separated by SiO_2 MPLC (100×460 mm; flow rate = 25 mL min^{-1}) eluted with *n*-hexane-EtOAc by gradually increasing the polarity system (from 100:0 to 0:100) to give ten fractions (Fr.1-10). Fr. 5 (15.6 g) was rechromatographed on reversed-phase (RP) MPLC (120 g; 75-140 μm ; 36×160 mm) eluted with an isocratic mobile phase ($\text{CH}_3\text{CN}-\text{MeOH}-\text{H}_2\text{O} = 4:3:3$) to furnish four fractions (Fr. 5.1–5.4). Fr. 5.4 (441 mg) was subjected into Sephadex LH-20 column chromatography (30 g; 20×450 mm) and followed by preparative RP-TLC purification (200×200 mm) with $\text{CH}_3\text{CN}-\text{MeOH}-\text{H}_2\text{O}$ (3:3:4) as mobile phase to give new compound **1** (6.0 mg). New compound **9** (3.7 mg) and 4-hydroxy-2,2,5-trimethyl-cyclopent-4-ene-1,3-dione (**16**, 3.6 mg) were obtained by purification of Fr. 5.3 with SiO_2 preparative TLC. Similarly, Fr. 3 (1.6 g) was rechromatographed by RP-MPLC, eluted with an isocratic mobile phase

(CH₃CN–MeOH–H₂O = 4:3:3, v/v) to yield seven fractions (Fr. 3.1–3.7). By purification using preparative RP-TLC with CH₃CN–MeOH–H₂O (3:3:4) as mobile phase, new compounds **2** (3.1 mg) and **3** (4.0 mg) were obtained from Fr. 3.2 (38 mg). Subfraction Fr. 3.1 (60 mg) was further subjected to SiO₂ preparative TLC (200 × 200 mm, 185 mm separation distance, *n*-hexane–EtOAc = 1:1), to afford a mixture of **4** and **5**, new compound **6** (1.3 mg), and an endoperoxide phloroglucinol (**14**, 20 mg). The mixture of **4** and **5** was then purified by SiO₂ HPLC (*n*-hexane–EtOAc = 50:50, v/v; flow rate = 2.0 mL min⁻¹; detection UV 254 nm), to provide new compounds **4** (10 mg) and **5** (1.5 mg). Furthermore, purification of Fr. 3.2 using SiO₂ preparative TLC was carried out to afford compound **7** (1.5 mg) and compound **8** (2.3 mg). Fr. 2 (2.3 g) was also rechromatographed on RP-MPLC eluted with an isocratic mobile phase CH₃CN–MeOH–H₂O (4:3:3) to give eight fractions (Fr. 2.1-2.8). Fr. 2.2 (94 mg) was further purified by preparative TLC with *n*-hexane–EtOAc (4:1) as mobile phase to furnish baeckeol (**13**, 20.5 mg), 5,7-dihydroxy-6,8-dimethylflavanone (**17**, 3.4 mg), and hybrid phloroglucinol (**20**, 381 mg). Moreover, new compound **12** (2.5 mg), a cyclopentenone derivative (**15**, 7 mg), a 5,7-dihydroxy-6-methylflavanone (**18**, 7 mg), and a humulene diepoxide (**21**, 10 mg) were isolated from Fr. 4 (1.2 g) by the similar procedure. On the other hand, Fr. 6 (5.9 g) was rechromatographed by MPLC over a silica gel eluting with a step gradient from 50 % to 80 % EtOAc in *n*-hexane to furnish four subfractions (Fr. 6.1–Fr. 6.4). Subfraction Fr. 6.2 was purified using Sephadex LH-20 and followed by preparative reversed-phase TLC developed with CH₃CN–MeOH–H₂O (4:3:3) to give new compound **10** (1.7 mg) and ursolic acid (**22**, 10 mg). Ursolic acid was found in most fractions since it was a major compound presence in this extract. Furthermore, Fr.1 (10.3 g) was subjected to silica gel

column chromatography eluting with a step gradient from 100% to 50% EtOAc in *n*-hexane to give four subfractions (Fr.1.1–Fr.1.4). Subfraction Fr.1.1 was further separated by ODS column chromatography and purified using SiO₂ preparative TLC (34 mg, *n*-hexane–EtOAc = 5:1), to afford new compound **11** (6 mg) and 5,7-dihydroxy-8-methyl-6-prenylated flavanone (**19**, 1.5 mg). All compounds were structurally elucidated using 1D and 2D NMR and MS spectra and compared with published data.

X-ray crystallographic analysis for baeckenone D (4)

X-ray data for compound **4** were collected on a Bruker APEX 2 CCD area detector diffractometer with a Helios multi-layered confocal mirror (ϕ - ω scans), using Mo *K* α radiation ($\lambda = 0.71069 \text{ \AA}$) from a Bruker TXS fine-focus rotating anode. The Bruker APEX 2 software was used for cell refinement and data reduction. The programs *SHELXS-97*, *SHELXL-2014*, and *PLATON* were used for the structure solution, the structure refinement, and the ORTEP plot, respectively.⁵⁶⁻⁵⁸ Crystallographic data for the structure of compound **4** have been preserved in the Cambridge Crystallographic Data Centre (deposition number: CCDC 1441723). Copies of these data can be obtained, free of charge, upon application to the Director, CCDC, 12 Union Road, Cambridge CB2 1EZ, UK (fax: +44-(0)1223-336033 or e-mail: deposit@ccdc.cam.ac.uk).

Crystal data of baeckenone D (**4**): C₁₅H₂₂O₅, *M* = 282.32, orthorhombic, space group *P2₁2₁2₁*, *a* = 10.5445(15) Å, *b* = 10.4510(15) Å, *c* = 27.954(4) Å, *V* = 3080.6(8) Å³, *Z* = 8, *D*_{calcd} = 1.217 g/cm³, *T* = 293 K, *F*(000) = 1216, and μ (Mo *K* α) = 0.091 mm⁻¹. A total of 9,344 reflections (1,738 unique, *R*_{int} = 0.0510) were collected from 1.46° to 21.36° in θ and index ranges $10 \geq h$

≥ -10 , $10 \geq k \geq -9$, $24 \geq l \geq -28$. The final stage converged to $R_1 = 0.0715$ ($wR_2 = 0.1972$) for 1,555 observed reflections [with $I > 2\sigma(I)$] and 188 variable parameters, and $R_1 = 0.0762$ ($wR_2 = 0.2009$) for all unique reflections, with GoF = 1.054.

Baeckenone A (1): Yellow amorphous powder; $C_{10}H_{14}O_3$; UV (MeOH) λ_{\max} : 208, 247, 288 nm; IR (KBr) ν_{\max} : 2928, 1660, 1541 cm^{-1} ; 1H and ^{13}C NMR: see Table 2.1; HREIMS m/z : 182.0937 $[M]^+$ (calcd. for $C_{10}H_{14}O_3$, 182.0943).

Baeckenone B (2): Yellow oil; $C_{25}H_{35}O_7$; $[\alpha]_D^{25}$ 0 (c 0.1, $CHCl_3$); UV (MeOH) λ_{\max} : 206, 233, 295 nm; IR (KBr) ν_{\max} : 3419, 2927, 1614 cm^{-1} ; 1H and ^{13}C NMR: see Table 2.2; HRESIMS m/z : 447.2383 $[M+H]^+$ (calcd. for $C_{25}H_{35}O_7$, 447.2383).

Baeckenone C (3): Yellow oil; $C_{30}H_{36}O_7$; $[\alpha]_D^{25}$ +21 (c 0.2, $CHCl_3$); IR (KBr) ν_{\max} : 3415, 2922, 1617 cm^{-1} ; 1H and ^{13}C NMR: see Table 2.2; HRESIMS m/z : 508.2461 $[M]^+$ (calcd. for $C_{30}H_{36}O_7$, 508.2479).

Baeckenone D (4): Colorless needles; MP 121–123 °C; $[\alpha]_D^{25}$ 0 (c 0.1, $CHCl_3$); UV (MeOH) λ_{\max} : 286 nm; IR (KBr) ν_{\max} : 3395, 2975, 1670, 1604, 1459 cm^{-1} ; 1H and ^{13}C NMR: see Table 2.3; HREIMS m/z : 282.1477 $[M]^+$ (calcd. for $C_{15}H_{22}O_5$, 282.1467).

Baeckenone E (5): White powder; $[\alpha]_D^{25}$ 0 (c 0.1, $CHCl_3$); UV (MeOH) λ_{\max} : 281 nm; IR (KBr) ν_{\max} : 3395, 2925, 1670, 1604, 1460 cm^{-1} ; 1H and ^{13}C NMR: see Table 2.3; HREIMS m/z : 282.1459 $[M]^+$ (calcd. for $C_{15}H_{22}O_5$, 282.1467).

Baectenone F (6): Yellow amorphous powder; $[\alpha]_{\text{D}}^{25} -44$ (*c* 0.1, CHCl₃); UV (MeOH) λ_{max} : 259 nm; IR (KBr) ν_{max} : 3444, 1668 cm⁻¹; ¹H and ¹³C NMR: see Table 2.4; HREIMS m/z : 254.1528 [M]⁺ (calcd. for C₁₄H₂₂O₄, 254.1518).

Frutescenenone A (7): Pale yellow amorphous powder; $[\alpha]_{\text{D}}^{25} +31$ (*c* 0.1, CHCl₃); UV (MeOH) λ_{max} : 233, 270 nm. IR (KBr) ν_{max} : 3421, 2926, 1740, 1609 cm⁻¹; ¹H and ¹³C NMR: see Table 2.5; HREIMS m/z : 228.1002 [M]⁺ (calcd. for C₁₁H₁₆O₅, 228.0998).

Frutescenenone B (8): Pale yellow amorphous powder; $[\alpha]_{\text{D}}^{25} +26$ (*c* 0.1, CHCl₃); UV (MeOH) λ_{max} : 257 nm. IR (KBr) ν_{max} : 3421, 1607 cm⁻¹; ¹H and ¹³C NMR: see Table 2.5. HREIMS m/z : 170.1528 [M]⁺ (calcd. for C₉H₁₄O₃, 170.1518).

Frutescenenone C (9): Pale yellow powder; UV (MeOH) λ_{max} : 221, 308 nm. IR (KBr) ν_{max} : 1752, 1699; ¹H and ¹³C NMR: see Table 2.6; HREIMS m/z : 236.1048 [M]⁺ (calcd. for C₁₃H₁₆O₄, 236.1049).

Baectenone G (10): Pale yellow amorphous powder; $[\alpha]_{\text{D}}^{25} +48$ (*c* 0.1, CHCl₃); UV (MeOH) λ_{max} : 238 nm; IR (KBr) ν_{max} : 3298, 1574 cm⁻¹; ¹H and ¹³C NMR: see Table 2.7; HREIMS m/z : 270.1110 [M]⁺ (calcd. for C₁₃H₁₈O₆, 270.1103).

Baectenone H (11): Pale yellow oil; $[\alpha]_{\text{D}}^{25} -52$ (*c* 0.1, CHCl₃); UV (MeOH) λ_{max} : 248, 271 nm; IR (KBr) ν_{max} : 3445 cm⁻¹; ¹H and ¹³C NMR: see Table 2.7; HREIMS m/z : 254.1163 [M]⁺ (calcd. for C₁₃H₁₈O₅, 254.1154).

Baeckenone I (12): White amorphous powder; $[\alpha]_D^{25}$ -16 (c 0.1, CHCl_3); UV (MeOH) λ_{max} : 248, 292 nm; IR (KBr) ν_{max} : 2916, 2849 cm^{-1} ; ^1H and ^{13}C NMR: see Table 2.8; HREIMS m/z : 266.1513 $[\text{M}]^+$ (calcd. for $\text{C}_{15}\text{H}_{22}\text{O}_4$, 266.1532).

IV. Experimental Detail of Chapter 3

Preparation of samples for antibacterial assay

5 mM stock sample solution was prepared in DMSO and further diluted to varied concentrations with YP medium in 96-well plates containing bacterial strains.

Cytotoxic assay

Cell viability in the presence or absence of the test compounds was determined using the standard WST-8 assay, as described previously. Briefly, the exponentially growing cells were harvested, and 2×10^3 cells were suspended in 100 μL of medium (α -MEM or DMEM at 37 $^\circ\text{C}$, under a 5% CO_2 and 95% air atmosphere) in each well of a 96-well plate. After the cells were incubated for 24 h and washed with PBS (Nissui Pharmaceuticals), serial dilutions of the samples to be tested were added. After a 72 h incubation at 37 $^\circ\text{C}$, the cells were washed with PBS, and 100 μL of α -MEM or DMEM containing 10% WST-8 cell counting kit solution (Dojindo; Kumamoto, Japan) was added to the wells. After a 2 h incubation at 37 $^\circ\text{C}$, the absorbance at 450 nm was measured. The concentrations of the serial dilutions of the tested samples were 100–3.125 μM for the isolated compounds and 10–0.3125 μM for the positive control. Cell viability was calculated from the mean values of data from three wells by using

the following equation, and cell viability was expressed as the IC₅₀ (50% inhibitory concentration) value.

$$(\%) \text{ Cell viability} = 100 \times \left[\frac{\text{Abs}_{(\text{test samples})} - \text{Abs}_{(\text{blank})}}{\text{Abs}_{(\text{control})} - \text{Abs}_{(\text{blank})}} \right]$$

Cell viability was presented as the 50% inhibitory concentration value. IC₅₀ values (concentration of inhibitory causing 50% reduction in activity relative to the control) were calculated by linear regression analysis of the inhibitor concentration versus percentage cell viability plots.

Preparation of the test samples for cytotoxic assay

10 mM stock solution was prepared by dissolving compounds in DMSO. Each solution was then applied to the 100 µL medium to produce a final concentration of 100–3.125 µM.

References

1. Ghosh, A.; Das, B. K.; Roy, A.; Mandal, B.; Chandra, G. Antibacterial activity of some medicinal plant extracts. *J. Nat. Med.* **2008**, *62*, 259–262.
2. Ekor, M. The growing use of herbal medicines: issues relating to adverse reactions and challenges in monitoring safety. *Front. Pharmacol.* **2013**, *4* (177), 1–10.
3. Navanesan, S.; Wahab, N. A.; Manickam, S.; Sim, K. S. Evaluation of selected biological capacities of *Baekea frutescens*. *BMC Complem. Altern. Med.* **2015**, *15*, 186.
4. Natural Products Isolation, 2nd edition. In *Methods in Biotechnology: 20*, edited by Satyajit D. Sarker, Zahid Latif, and Alexander I. Gray, 2005.
5. Herdiyeni, Y.; Adisantoso, J.; Damayanti, E. K.; Zuhud, E. A. M.; Douady, S (Eds.). Indonesian Tropical Medicinal Plants Diversity: Problems and Challenges in Identification. *Proceeding of 2011 International Workshop “Linking Biodiversity and Computer Vision Technology to Enhance Sustainable Utilization of Indonesian Tropical Medicinal Plants”*. 2011, IPB Darmaga, Bogor.
6. Cowan, M. M. Plant products as antimicrobial agents. *Clin. Microbiol. Rev.* **1999**, *12* (4), 564–582.
7. Alavijeh, P. K.; Alavijeh, P. K.; Sharma, D. A study of antimicrobial activity of few medicinal herbs. *Asian J. Plant Sci. Res.* **2012**, *2*, 496–502.
8. Balouiri, M.; Sadiki, M.; Ibsouda, S. K. Methods for *in vitro* evaluating antimicrobial activity: A review. *J. Pharm. Anal.* **2016**, *6*, 71–79.

9. Evans, C. E.; Bansa, A.; Samuel, A. O. Efficacy of some nupe medicinal plants against *Salmonella typhi*: an in vitro study. *J. Ethno. Pharmacology*. **2002**, 80, 21–24.
10. Parekh, J.; Chanda, S. Antibacterial and phytochemical studies on twelve species of Indian medicinal plants. *Afr. J. Biomed. Res.* **2007**, 10, 175–181.
11. Silver, L. L. Challenges of antibacterial discovery. *Clin. Microbiol. Rev.* **2011**, Jan, 71–109
12. Yu Jun, S.; Chen, J.; Xu, M. A new method for antimicrobial susceptibility testing of *Vitro*-cultured bacteria by means of Resonance Light Scattering technique. *J. Microbiol. Biotechnol.* **2008**, 18, 118–123.
13. Mosmann, T. Rapid colorimetric assay for cellular growth and survival: Application to proliferation and cytotoxicity assays. *J. Immunol. Methods.* **1983**, 65, 55–63.
14. Malekinejad, H.; Gilani, B. B.; Tukmechi, A.; Ebrahimi, H. A cytotoxicity and comparative antibacterial study on the effect of *Zataria multiflora* Boiss, *Trachyspermum copticum* essential oils, and Enrofloxacin on *Aeromonas hydrophila*. *Avicenna J. Phytomed.* **2012**, 2, 188–195.
15. Delcour, A. H. Outer Membrane Permeability and Antibiotic Resistance. *Biochim. Biophys. Acta.* **2009**, 1794, 808–816.
16. Bean, A. R. A Revision of *Baeckea* (Myrtaceae) in eastern Australia, Malesia and South-east Asia. *Telopia.* **1997**, 7, 245–268.
17. Mardisiswojo, S. Cabe Puyang Warisan Nenek Moyang. PN Jakarta, Balai Pustaka. **1985**, 95.

18. Ahmad, N. S.; Ghani, M. N.; Ali, A. M.; Johari, S. T.; Harun, M. H. High Performance Liquid Chromatography (HPLC) profiling analysis and bioactivity of *Baeckea frutescens* L. (Myrtaceae). *J. Med. Plants Stud.* **2012**, 1, 101–108.
19. Murnigsih, T.; Subeki.; Matsuura, H.; Takahashi, K., Yamasaki, M.; Yamato, O.; Yoshimitsu, M.; Katakura, K.; Suzuki, M.; Kobayashi, S.; Chairul.; Yoshihara, T. J. Evaluation of the inhibitory activities of the extracts of Indonesian traditional medicinal plants against *Plasmodium falciparum* and *Babesia gibsoni*. *Vet. Med. Sci.* **2005**, 67, 829–831.
20. Tsui, W. Y.; Brown, G. D. Unusual metabolites of *Baeckea frutescens*. *Tetrahedron* **1996**, 52, 9735–9742.
21. Sunarti, S. Jungrahab (*Baeckea frutescens* L.): satu-satunya tumbuhan obat dari marga *Baeckea* di Indonesia dan koleksinya di herbarium Bogoriense. *Majalah Obat Tradisional* **2008**, 13, 167–171.
22. Dai, D. N.; Thang, T. D.; Olayiwola, T. O.; Ogunwande, I. A. Chemical composition of essential oil of *Baeckea frutescens* L. *Int. Res. J. Pure Appl. Chem.* **2015**, 8(1), 26–32.
23. Tam, N. T.; Thuam, D. T.; Bighelli, A.; Castola, V.; Muselli, A.; Richomme, P.; Casanova, J. *Baeckea frutescens* leaf oil from Vietnam: composition and chemical variability. *Flavour Fragr. J.* **2004**, 19, 217–220.
24. Fujimoto, Y.; Usui, S.; Makino, M.; Sumatra, M. Phloroglucinols from *Baeckea frutescens*. *Phytochemistry* **1996**, 41, 923–925.

25. Jia, B. X.; Zeng, X. L.; Ren, F. X.; Jia, L.; Chen, X. Q.; Yang, J.; Liu, H. M.; Wang, Q. Baeckeins F–I, four novel C-methylated biflavonoids from the roots of *Baeckea frutescens* and their anti-inflammatory activities. *Food Chem.* **2014**, 155, 31–37.
26. Makino, M.; Fujimoto, Y. Flavanones from *Baeckea frutescens*. *Phytochemistry* **1999**, 50, 273–277.
27. Kamiya, K.; Satake, T. Chemical constituents of *Baeckea frutescens* leaves inhibit copper-induced low-density lipoprotein oxidation. *Fitoterapia* **2010**, 81, 185–189.
28. Nisa, K.; Ito, T.; Subehan.; Matsui, T.; Kodama, T.; Morita, H. New acylphloroglucinol derivatives from the leaves of *Baeckea frutescens*. *Phytochem. Lett.* **2016**, 15, 42–45.
29. Nisa, K.; Ito, T.; Kodama, T.; Tanaka, M.; Okamoto, Y.; Asakawa, Y.; Imagawa, H.; Morita H. New cytotoxic phloroglucinols, baeckenones D–F, from the leaves of Indonesian *Baeckea frutescens*, *Fitoterapia* **2016**, 109, 236–240
30. Ito, T.; Nisa, K.; Kodama, T.; Tanaka, M.; Okamoto, Y.; Ismail.; Morita, H. Two new cyclopentenones and a new furanone from *Baeckea frutescens* and their cytotoxicities. *Fitoterapia* **2016**, 112, 132–135
31. Jia, B. X.; Yang, J.; Chen, X. Q.; Cao, Y.; Lai, M. X.; Wang, Q. Baeckeins A and B, two novel 6-Methylflavonoids from the roots of *Baeckea frutescens*. *Helv. Chim. Acta.* **2011**, 94, 2283–2288.
32. Jia, B. X.; Zhou, Y. X.; Chen, X. Q.; Wang, X. B.; Yang, J.; Lai, M. X.; Wang, Q. Structure determination of baeckeins C and D from the roots of *Baeckea frutescens*. *Magn. Reson. Chem.* **2011**, 49, 757–761.

33. Tsui, W. Y.; Brown, G. D. Sesquiterpenes from *Baeckea frutescens*. *J. Nat. Prod.* **1996**, *59*, 1084–1086.
34. Tsui, W. Y.; Brown, G. D. Chromones and chromanones from *Baeckea frutescens*. *Phytochemistry* **1996**, *43*, 871–876.
35. Buyk, L. D.; Verhé, R.; Kimpe, N. D.; Courtheyn, D.; Schamp, N. Alternative syntheses of 3,3,5-Trimethyl-1,2,4-Cyclopentanetrione. *Bull. Soc. Chim. Belges.* **1981**, *90*, 837–846.
36. Coutinho, I. D.; Coelho, R. G.; Kataoka, V. M. F.; Honda, N. K.; Silva, J. R. M.; Vilegas W.; Cardoso, C. A. L. Determination of phenolic compounds and evaluation of antioxidant capacity of *Campomanesia adamantium* leaves. *Ecl. Quím. São Paulo* **2008**, *33*, 53–60.
37. Fang, J.; Paetz, C.; Schneider, B. C-methylated flavanones and dihydrochalcones from *Myrica gale* seeds. *Biochem. Syst. Ecol.* **2011**, *39*, 68–70.
38. Furusawa, M.; Ido, Y.; Tanaka, T.; Ito, T.; Nakaya, K.; Ibrahim, I.; Ohyama, M.; Iinuma, M.; Shirataka, Y.; Takahashi, Y. Novel, complex flavanoids from *Mallotus philippensis* (Kamala Tree). *Helv. Chim. Acta*, **2005**, *88*, 1048–1058.
39. Kaouadji, M.; Ravanel, P.; Mariotte, A. M. New prenylated flavanones from *Platanus acerifolia* Buds. *J. Nat. Prod.* **1986**, *49*, 153–155.
40. Cradwick, M. E.; Cradwick, P. D.; Sim, G. A. Sesquiterpenoids. Part XV. Conformation of humulene: X-ray analysis of the crystal structure of humulene diepoxide. *J. Chem. Soc. Perkin Trans 2* **1973**, *2*, 404–407.
41. Jin, Q.; Fang, H. Z., Jun, L. Z., Yang, Y. B. Triterpenes from *Prunella vulgaris*. *Chin. J. Nat. Med.* **2009**, *7*, 421–424.

42. Seebacher, W.; Simic, N.; Weis, R.; Saf, R.; Kunert, O. Spectral assignments and reference data: Complete assignments of ^1H and ^{13}C NMR resonances of oleanolic acid, 18a-oleanolic acid, ursolic acid and their 11-oxoderivatives. *Magn. Reson. Chem.* **2003**, 41, 636–638.
43. Takasaki, M.; Konoshima, T.; Etoh, H.; Singh, I. P.; Tokuda, H.; Nishino, H. Cancer chemopreventive activity of euglobal-G1 from leaves of *Eucalyptus grandis*. *Cancer Lett.* **2000**, 155, 61–65.
44. Singh, I. P.; Bharate, S. B. Phloroglucinol compounds of natural origin. *Nat. Prod. Rep.* **2006**, 23, 558–591.
45. Osawa, K.; Yasuda, H.; Morita, H.; Takeya, K.; Itokawa, H. Eucalyptone from *Eucalyptus globulus*. *Phytochemistry* **1995**, 40, 183–184.
46. Win, N.N.; Ito, T.; Aimaiti, S.; Kodama, T.; Imagawa, H.; Ngwe, H.; Asakawa, Y.; Abe, I.; Morita, H. Kaempulchraols I–O: new isopimarane diterpenoids from *Kaempferia pulchra* rhizomes collected in Myanmar and their antiproliferative activity. *Tetrahedron* **2015**, 71, 4707–4713.
47. Yang, F.; Cao, Y. Biosynthesis of phloroglucinol compounds in microorganisms—review. *Appl. Microbiol. Biotechnol.* **2012**, 93, 487–495.
48. Nagpal, N.; Shah, G.; Arora, M. N. Shri, R.; Arya, A. Phytochemical and pharmacological aspects of *Eucalyptus* genus. *Int. J. Pharm. Sci. Res.* **2010**, 12, 28–36.
49. Ghisalberti E. L. Bioactive acylphloroglucinol derivatives from *Eucalyptus* species, *Phytochemistry* **1996**, 417–422.

50. Singh, I. P.; Etoh, H. Biological activities of phloroglucinol derivatives from *Eucalyptus* species. *Nat. Prod. Sci.* **1997**, 3, 1–7.
51. Sidana, J.; Singh, S.; Arora, S. K.; Foley, W. J.; Singh, I. P. Formylated phloroglucinols from *Eucalyptus loxophleba* foliage. *Fitoterapia* **2011**, 82, 1118–1122.
52. Wang, J.; Zhai, W. Z.; Zou, Y.; Zhu, J. J.; Xiong, J.; Zhao, Y.; Yang, G. X.; Fan, H.; Hamann, M. T.; Xia, G.; Hua, J. F. Eucalyptals D and E, new cytotoxic phloroglucinols from the fruits of *Eucalyptus globulus* and assignment of absolute configuration. *Tetrahedron Lett.* **2012**, 53, 2654–2658.
53. Soliman, F. M.; Fathy, M. M.; Salama, M. M.; Al-Abd, A.M.; Saber, F. R.; El-Halawany, A. M. Cytotoxic activity of acyl phloroglucinols isolated from the leaves of *Eucalyptus cinerea* F. Muell. ex Benth. cultivated in Egypt. *Sci. Rep.* **2014**, 4, 5410.
54. Iskra, J. Antimalarial peroxides: from artemisinin to synthetic peroxides. *Antimalarial Drugs* **2009**, 141–182.
55. Najjar, F.; Baltas, M.; Gorrichon, L.; Moreno, Y.; Tzedakis, T.; Vial, H.; Andre-Barres, C. Synthesis and electrochemical studies of new antimalarial endoperoxides. *Eur. J. Org. Chem.* **2003**, 17, 3335–3343.
56. Sheldrick, G. M. SHELXS-97, Program for crystal structure solution; University of Göttingen: Germany, **1997**.
57. Sheldrick, G. M. SHELXL-2014, Program for structure refinement; University of Göttingen, Germany, **2014**.
58. Spek, A. Structure validation in chemical crystallography. *Acta Crystallogr.* **2009**, D65, 148–155.

List of publications

This doctoral thesis summarizes the full contents of the following publications.

- 1) **Nisa, K.**; Ito, T.; Subehan.; Matsui, T.; Kodama, T.; Morita, H. New acylphloroglucinol derivatives from the leaves of *Baeckea frutescens*. *Phytochemistry Letter* **2016**, 15, 42–45.
- 2) **Nisa, K.**; Ito, T.; Kodama, T.; Tanaka, M.; Okamoto, Y.; Asakawa, Y.; Imagawa, H.; Morita, H. New cytotoxic phloroglucinols, baeckenones D–F, from the leaves of Indonesian *Baeckea frutescens*. *Fitoterapia* **2016**, 109, 236–240.
- 3) Ito, T.; **Nisa, K.**; Kodama, T.; Tanaka, M.; Okamoto, Y.; Ismail.; Morita, H. Two new cyclopentenones and a new furanone from *Baeckea frutescens* and their cytotoxicities. *Fitoterapia* **2016**, 112, 132–135.

Acknowledgments

I wish to express my deepest and sincere gratitude to my supervisor Prof. Dr. Hiroyuki Morita, Division of Natural Products Chemistry, Institute of Natural Medicine, University of Toyama, for his valuable instruction, guidance, and suggestion to achieve my PhD course. I am highly grateful to Associate Prof. Dr. Takuya Ito, Division of Natural Products Chemistry, Institute of Natural Medicine, University of Toyama, for his expert guidance, generous support, and kindness to my study and life in Toyama. I would like to express my thanks to Assistant Prof. Takashi Matsui, for his kindly help, attention, and support during my three years study.

I would like to express my appreciation to Dr. Subehan Ambo Lallo, Faculty of Pharmacy, University of Hasanuddin, for his assistance and suggestion in the beginning of my study.

I would like to acknowledge my sincere thanks to Ministry of Research, Technology and Higher Education of the Republic of Indonesia for a scholarship and financial support.

I would like to thank all staffs of Research Unit of Natural Product Technology, Indonesian Institute of Sciences for their support, caring, and encouragement.

I would like to express my special thank to all members in Division of Natural Products Chemistry for the great support and kind help during my study in the University of Toyama.

Finally, I am greatly indebted to my family especially my mother, my husband and my sons for their love, understanding, support, and encouragement.